HHS Public Access

Author manuscript

Dev Biol. Author manuscript; available in PMC 2021 January 01.

Published in final edited form as:

Dev Biol. 2020 January 01; 457(1): 150–162. doi:10.1016/j.ydbio.2019.10.002.

Yap/Taz are required for establishing the cerebellar radial glia scaffold and proper foliation

Lucinda J. Hughes[1,2], **Raehee Park**[1], **Min Jung Lee**[1], **Bethany K. Terry**[1,2], **David J. Lee**[1], **Hansol Kim**[1], **Seo-Hee Cho**[1], **Seonhee Kim**[1,*]

[1]Shriners Hospitals Pediatrics Research Center, Department of Anatomy and Cell Biology

[2]Graduate Program of Biomedical Sciences, Temple University Lewis Katz School of Medicine, Philadelphia, PA, 19140

Abstract

Yap/Taz are well-established downstream effectors of the Hippo pathway, known to regulate organ size by directing proliferation and apoptosis. Although the functions of Yap/Taz have been extensively studied, little is known about their role in brain development. Here, through genetic ablation, we show that Yap/Taz are required for cerebellar morphogenesis. Yap/Taz deletion in neural progenitors causes defects in secondary fissure formation, leading to abnormal folia development. Although they seemed very likely to serve an important function in the development of cerebellar granule cell precursors, Yap/Taz are dispensable for their proliferation. Furthermore, Yap/Taz loss does not rescue the medulloblastoma phenotype caused by constitutively active Smoothened. Importantly, Yap/Taz are highly expressed in radial glia and play a crucial role in establishing the radial scaffold and cellular polarity of neural progenitors during embryogenesis. We found that Yap/Taz are necessary to establish and maintain junctional integrity of cerebellar neuroepithelium as prominent junction proteins are not maintained at the apical junction in the absence of Yap/Taz. Our study identifies a novel function of Yap/Taz in cerebellar foliation and finds that they are required to establish the radial glia scaffold and junctional stability.

INTRODUCTION

Hippo-Yap signaling is a well-described pathway that regulates cell fate, proliferation, and apoptosis. First described in *Drosophila melanogaster*, its components are well conserved in mammals (Hong and Guan, 2012). The core cassette contains the serine/threonine kinases Hippo (Hpo) and Warts (Wts), with mammalian homologues MST1/2 and LATS1/2, respectively (Harvey and Hariharan, 2012). The downstream effector protein Yorkie (Yki) and vertebrate homologues Yap/Taz are phosphorylated upon pathway activation, inhibiting

*Correspondence should be addressed to: Dr. Seonhee Kim, Shriners Hospitals Pediatrics Research Center, Department of Anatomy and Cell Biology, Temple University Lewis Katz School of Medicine, 3500 North Broad St. Philadelphia, PA, 19140, seonhee.kim@temple.edu.

Conflict of Interest: The authors declare no competing financial interests.

their function as transcriptional co-activators by promoting cytoplasmic retention, 14–3-3 binding, and degradation (Varelas, 2014; Zhao et al., 2010). Yap subcellular localization is influenced by a variety of cues including cell density (Zhao et al., 2010), extracellular lipids such as lysophosphatidic acid (LPA) and sphingosine-1-phosphate (S1P) (Yu et al., 2012), and mechanical tension (Calvo et al., 2013). Injury and tumorigenic cues are also known to induce Yap translocation and subsequent transcription of target genes (Johnson and Halder, 2014). It is well-established that Yap is important for organ size control (Halder et al., 2012) and cell and regional fates (Hao et al., 2014; Kim et al., 2016) in various organ systems. Its abnormal expression is linked to cortical malformations such as periventricular heterotopia and subcortical heterotopia (Cappello et al., 2013; Liu et al., 2018b). However, the normal function of Yap/Taz in brain development, including the cerebellum, remains largely unknown.

Stepwise and precise generation of different cell types, establishment of three cortical layers, and organization of the cortex into distinct folia are essential for proper formation of the cerebellum (Roussel and Hatten, 2011). Purkinje cells (PC), interneurons, and neurons of the cerebellar nuclei arise from the ventricular zone (VZ), which comprises neural progenitors with epithelial characteristics. The processes of neural progenitors form a radial scaffold, which supports the shape of the embryonic cerebellum and migration of PCs and other cells. Neural progenitors in the VZ transform to Bergman glia (BG) and migrate to the PC layer (PCL) during late embryogenesis and early postnatal stages (Buffo and Rossi, 2013). Long BG radial processes span the molecular layer (ML) and contact the basement membrane (BM) beneath the pia, providing a scaffold for maturing granule cells to migrate along from the external granular layer (EGL) to the inner granule layer (IGL). Furthermore, PCs, BG, and granule cells are important for cerebellar foliation by forming ‘anchoring centers’, thereby establishing the base of the characteristic cerebellar fissures (Sudarov and Joyner, 2007). Although these important morphogenetic and scaffolding roles of neural progenitors and BG have been identified, the molecules and signaling pathways necessary for their proper development are less well understood.

Cerebellar granule neuron precursors (CGNPs), which do not exhibit epithelial polarity, migrate from the upper rhombic lip (URL), a germinal zone located between the cerebellar anlage and choroid plexus, to form the EGL. Postnatally, CGNPs extensively proliferate in response to Sonic Hedgehog (Shh) secreted by PCs, and then differentiate and migrate inward via BG fibers to form the IGL (Roussel and Hatten, 2011).

In addition to its role in organogenesis, Yap has also been implicated in several different cancer types where it is found aberrantly upregulated (Johnson and Halder, 2014; Liu et al., 2018a; Moon et al., 2018), including medulloblastoma, a tumor of the cerebellum of which at least the Shh-mediated subtype is believed to arise from granule neuron precursors (Fernandez et al., 2009; Orr et al., 2011). Previous studies demonstrated that Shh upregulates and stabilizes Yap (Fernandez et al., 2009), and that Yap-dependent expression of Y-box binding protein-1 (YB-1), which increases insulin-like growth factor 2 expression, drives CGNP proliferation in culture (Dey et al., 2016). Despite the observation of increased Yap in medulloblastoma (Orr et al., 2011) and its role in tumor radioresistance (Fernandez et al., 2009), the significance of Yap/Taz in the establishment of cerebellar tumors is unknown.

The present study describes the expression pattern of Yap in the developing cerebellum and demonstrates a novel function of Yap/Taz in the timely establishment of secondary fissures required for normal foliation. In the absence of Yap/Taz, embryonic CGNPs are reduced in number and the radial scaffold of radial glia progenitors (RGPs) is disrupted and accompanied by a thinned embryonic cerebellum. However, we found that Yap/Taz are dispensable for postnatal expansion of CGNPs and have a minimal role in cerebellar tumorigenesis caused by constitutively active Smoothened. Importantly, we identify the essential role of Yap/Taz in junctional integrity and cell polarity of radial glia progenitors through proper localization of adherens junction proteins, apical polarity complex proteins, and non-muscle myosin IIB (NMIIB) at the apical junction, which is required for cerebellar morphogenesis.

Materials and Methods

Mice

All experiments with animals were conducted in accordance with protocols approved by the IACUC of Temple University Lewis Katz School of Medicine. *Yap*$^{f/f}$ and *Taz*$^{f/f}$ were obtained from Dr. Olson (UT Southwestern Medical School, Dallas) (Xin et al., 2013). *Yap*$^{f/f}$ and *Taz*$^{f/f}$ mice were bred to generate *Yap*$^{f/f}$/*Taz*$^{f/f}$, which were then bred to *Nestin-Cre* (Dubois et al., 2006), *hGFAP-Cre* (Zhuo et al., 2001), *mGFAP-Cre* (77.6) (Gregorian et al., 2009) or *Math1-Cre* (Matei et al., 2005) mice from The Jackson Laboratory. Progeny were genotyped by PCR for *Yap* as previously described (Song et al., 2014). *Taz* and *SmoM2* (from The Jackson Laboratory) were genotyped by PCR using two primers (*Taz*: Forward 5' CTCATATCCAAAGGCTGACTAA, Reverse 5' ATGTTACGATGAGGAACTCTTC; *SmoM2:* Forward 5' AAGTTCATCTGCACCACCC, Reverse 5' TGCTCAGGTAGTGGTTGTCG). The reporter mouse line was ROSA$^{mT/mG}$ (Muzumdar et al., 2007) from The Jackson Laboratory. *Yap*$^{f/f}$ and *Taz*$^{f/f}$ were maintained on a mixed genetic background of C56BL6 and 129. To generate CKOs, mice with floxed alleles were crossed with Cre drivers maintained on various backgrounds by The Jackson Laboratory.

Histology and immunohistochemistry

Embryonic mice were decapitated and heads were fixed in 4% paraformaldehyde (PFA) in PBS at 4°C overnight. Postnatal animals were perfused and brains were dissected out, then fixed in 4% PFA in PBS at 4°C overnight. Parasagittal sections 7μm thick were prepared from fixed tissues embedded in paraffin. Hematoxylin and eosin (H&E), immunofluorescence, and immunohistochemical staining of tissue sections were performed as previously described (Park et al., 2016a; Park et al., 2016b). Antibodies used were Yap (1:500; abcam ab56701), BLBP (1:200; Millipore ABN14), Calbindin (1:200; Sigma, C9848), S100β (1:200; Novus Biologicals, NB110–57478), GFAP (1:200; Thermo Scientific, RB-087), BrdU (1:500; abcam, ab6326), PCNA (1:250; Proteintech, 10205–2-P), pH3 (1:500; Millipore Sigma, 06–670), NeuN (1:250; Millipore, MAB377), Pax6 (1:200; Covance, RBP-278), Sox9 (1:200; Millipore, AB5535), Pals1 (1:200; Proteintech), Pan-Crb (1:200; (Cho et al., 2012)), NMIIB (1:500; Covance, PRB-445P), N-Cadherin (1:500; BD, 610920), and β-Catenin (1:500; BD, 610153). Species-specific secondary antibodies

conjugated to Alexa Fluor 488 (1:250; Invitrogen) or Cy3 (1:250; Jackson Immunochemical) were used for immunofluorescence. Nuclei were stained with Hoechst 22358 (1:500; Invitrogen).

Measurements and cell number quantification

Fissure length was defined as the distance from the base of the precentral fissure perpendicular to a line tangential to the crowns of lobules II and III, and measured using ImageJ (n=3, four midsagittal sections per animal). To count the number of PCs and the number of BG in PCL or ML, the number of Calbindin$^+$ and S100β$^+$ cells, respectively, were manually counted using Photoshop at one to two midsagittal sections per animal (n>3). Length of the cerebellum and PCL was calculated using ImageJ. To determine the number of pH3$^+$ cells in the embryonic cerebellum, pH3$^+$ cells were manually counted using Photoshop at two midsagittal sections per animal (n=3 or more). To compare the fraction of BrdU$^+$ cells among total PCNA$^+$ proliferating cells in the URL and EGL in the embryonic cerebellum, the number of PCNA$^+$ cells and PCNA$^+$ BrdU$^+$ cells were manually counted using Photoshop at one midsagittal section per animal (n=4 WT and n=5 dCKO). Length of the lobes was calculated using ImageJ. To obtain the fraction of BrdU$^+$ cells in the EGL, the number of BrdU$^+$ cells and total Hoechst$^+$ cells were manually counted over 100 μm in the EGL of lobule III (crown area) using 40X images taken from confocal microscopy (Leica, TCS SP8). Cells were counted using Photoshop at two midsagittal sections per animal (n=3 or more).

Western blot analyses

Whole cerebellums from P0 Yap/Taz dCKO or Yap heterozygote/Taz CKO with Nestin-Cre and littermate control mice (Cre$^-$) were lysed to obtain protein for Western blot analysis as previously described (Park et al., 2016b). Briefly, proteins were separated on an SDS-PAGE gel and transferred to a polyvinylidene difluoride membrane. After blocking with 5% nonfat dry milk, the membrane was incubated with primary antibodies Yap (1:1000; Abcam ab56701), Taz (1:1000; V386 Cell signaling), Pals1 (1:1000; Proteintech, 17710–1-AP), β-Catenin (1:1000; BD, 610153), NMIIB (1:2000; Covance, PRB-445P), N-Cadherin (1:1000; BD, 610920) and GAPDH (1:4000; Proteintech 60004–1-Ig and 10494–1-AP). Protein signals were detected using chemiluminescence (ECL Kit, GE Healthcare).

Granule cell isolation

Granule cells from *Yap*$^{f/f}$*Taz*$^{f/f}$;*Nestin-Cre, Yap*$^{f/f}$*Taz*$^{f/f}$;*Math1-Cre* and WT littermates (Cre$^-$) were isolated at P7 with a papain dissociation kit (Worthington Biomedical) as described previously (Lee et al., 2009). For GNP proliferation analysis, purified GNPs were plated on poly-D-lysine coated chamber slides (Nunc). The cells were grown in neurobasal medium with B-27 supplement (Gibco), with or without mouse Shh (3mg/ml, Novus biologicals). After 24 hrs of incubation, BrdU (3mg/ml) was added to the medium for 4 hrs. Cells were then fixed with 4 % PFA for 10 min and washed with PBS. Primary antibodies (α-Yap, α-Pax6, α-BrdU) were added with 5% Goat serum in PBS. For BrdU detection, cells were incubated with 2N HCl for 30 min at 37°C prior to primary antibody application. Secondary antibodies were used as described above.

Statistical analysis

To determine statistical significance for fissure length and for cell counting of PCs, BG, M-phase ($pH3^+$), S-phase ($BrdU^+$), and $Hoechst^+$ nuclei, an F-test was performed to determine if the variances were equal or unequal prior to applying the appropriate two-tailed t-test. Statistical analyses were performed using Excel (Microsoft) or SigmaPlot (Systat Software) and significance was determined as $p<0.05$.

RESULTS

Yap is expressed in progenitor cells and glia cells in the developing cerebellum

The Hippo/Yap pathway has been the focus of many studies of organ systems in recent years, although relatively little is yet known about its role in the CNS, particularly in the cerebellum. To establish the expression pattern of Yap in the developing mouse cerebellum, we examined midsagittal sections at the vermis by immunofluorescence at various ages from the embryonic stage through adulthood. Yap is consistently highly expressed in the choroid plexus (CP) and meninges, which served as positive controls for Yap staining in our subsequent conditional knockout (CKO) experiments. By E12.5, Yap is highly expressed in the cytoplasm of $Sox9^+$ progenitor cells in the VZ and a subset of their nuclei but is nearly undetectable in $Sox9^-$ postmitotic cells located closer to the pia membrane (Fig. 1A). At E16.5, Yap expression in proliferating cells remains high and is evident in the VZ demarcated by brain lipid-binding protein $(BLBP)^+$ radial glia cells, the URL, and the emerging EGL labeled by Pax6 (Fig. 1B). Yap expression is detected in both the nucleus and cytoplasm of EGL, URL and VZ progenitors. Yap is also apparent in radial glia processes labelled by BLBP (Fig. 1C). At birth (P0), Yap expression persists in $Pax6^+$ cells in the outer most layers of the EGL (oEGL) (Fig. 1D) and is found in cells in the PCL, white matter, and ventricular lining cells of the fourth ventricle (Fig. 1D). Yap expression shows a graded distribution (anterior high and posterior low) in the emerging PCL (Fig. S1A), correlating with the accumulation of $S100\beta^+$ BG at the PCL in the anterior lobes. By P5, Yap continues to be highly expressed in the BG soma, including the nucleus and radial processes (Fig. 1E, F), but is notably absent from PCs (Fig. 1G). P5 marks the beginning of the peak postnatal CGNP proliferation period, and Yap remains evident in the oEGL, limited to 1–2 cell layers from the meninges (Fig. 1D). Yap expression in BG processes was also confirmed by extensively overlapping Yap and GFAP immunostaining at P7 (Fig. S1B). Yap expression is undetectable in the EGL at P14 when most EGL cells are postmitotic, supporting that it is expressed in the EGL by proliferating CGNPs (Fig. S1C). Yap expression in the BG also gradually declines and by P21, Yap protein is weakly detected by immunofluorescence (Fig. S6E). However, enhanced staining using DAB (3, 3'-diaminobenzidine) confirmed the presence of Yap in at least a subset of BG in the adult cerebellum; similar staining is not detectable in the *Yap* CKO; *hGFAP-Cre* mice (Fig. 1H). The spatial and temporal dynamics of Yap expression suggests that Yap may have a function in the proliferation of neural progenitors, including radial glia progenitors and CGNPs, and its persistent expression in BG raises the possibility that it may play a role in BG development and function.

Loss of Yap/Taz in the cerebellum causes folia defects

In order to determine the function of Yap/Taz in the developing cerebellum, we conditionally knocked out both *Yap* and *Taz* by crossing $Yap^{f/f};Taz^{f/f}$ mice with *Nestin-Cre* mice (Dubois et al., 2006), which deleted *Yap* and *Taz* in glial cells and neurons throughout the CNS. These mutant mice exhibited hydrocephalus and an undersized cerebellum at birth. While the four principal fissures are apparent in the WT and in most of the *Yap/Taz* dCKO cerebellums at P0 (Fig. 2A, B, asterisks), the posterolateral principal fissure is less distinct in some early postnatal dCKO animals (Fig. 2D, asterisk). The most consistent feature found in the dCKO is the absence of the cell lining of the fourth ventricle (Fig. 2A, B). At P3, while the precentral fissure between lobules II and III is distinctively established in WT, there is no sign of the fissure in the dCKO (Fig. 2C, D). However, at P7, the precentral fissure is noticeable in the dCKO, demonstrating that fissure formation is delayed in the absence of Yap/Taz (Fig. 2E, F, arrows). As development proceeds, the notable foliation defects remain at P10 (Fig. 2G, H) and thereafter. To characterize the degree of foliation defects, we compared precentral fissure depth in WT and dCKO at P10 (Fig. 2G, H). The depth of the dCKO fissure was significantly shorter than that of the WT, and fissure length was four-fold shorter in the dCKO than the WT (Fig. 2I). At P21, *Yap/Taz* dCKO mice had prominent foliation defects, including the shortened precentral fissure (Fig. 2J, K). In addition to precentral fissure defects, folia VIa and VIb were not clearly separated in the mutant, and folium IX was also underdeveloped with a missing uvular sulcus (US) (Fig. 2J, K). Taken together, Yap/Taz function is required for proper folia formation during development.

Yap/Taz are required for embryonic cerebellar shape and size

Proper foliation involves coordinated interaction among CGNPs, PCs, and BG (Sudarov and Joyner, 2007). To detect earlier deficits responsible for the cerebellar folia phenotype in the *Yap/Taz* dCKO, we have closely examined progenitors generating these cell types during embryogenesis. At E13.5, the expression of Yap in the dCKO cerebellum is nearly undetectable while all three germinal zones express Yap in the WT (Fig. 3A, B). Although we did not detect obvious gross morphological changes in the cerebellar anlage at E13.5, the URL is smaller than that of WT (Fig. 3B). To examine the proliferative capacity of cells in the URL marked by proliferating cell nuclear antigen (PCNA), we determined the proportion of cells in S-phase among total $PCNA^+$ cells (Fig. 3C–F). S-phase cells are labeled by injecting BrdU into the pregnant dam 30 minutes prior to the collection of embryos. Despite a striking reduction in the number of cells in the URL, we did not observe any statistically significant differences in proliferative capacity between WT and dCKO (Fig 3G, H). When we next compared the proliferation of Pax6+ cells in the EGL, which are mainly $PCNA^+$ proliferating cells (Fig. 3C,D), we again found the fraction of S-phase cells among total $PCNA^+$ proliferating EGL cells to be unaffected (Fig. 3I). These results suggest that despite the small size of the URL, cell proliferation of URL and EGL is not compromised at this stage.

Unlike at E13.5, when dCKO cerebellum size is indistinguishable from WT, at E16.5 the cerebellum of *Yap/Taz* dCKO is slender and undersized, and Yap expression remains undetectable (Fig. 3J). To characterize the extent of cerebellar shape changes, we measured the width and length of the cerebellum at the midsagittal section at E16.5 (Fig. 3K). The

width of the cerebellum is remarkably reduced compared to that of WT littermates and, although less striking, cerebellar length is also significantly decreased (Fig. 3K, N, O). Because we observed the size of the URL to be reduced at E13.5 and still undersized at E16.5, but did not observe compromised proliferation of URL and EGL cells at E13.5, we determined the population of $Pax6^+$ CGNPs and CGNs in the midsagittal section at E16.5. We found a statistically significant reduction of $Pax6^+$ cells in the dCKO compared to WT (Fig. 3P). Since proliferation was not reduced at E13.5 and the thickness of EGL at E16.5 appears to be unaffected (Fig. 3L), we reasoned that the proliferation of CGNPs in the EGL might also not be altered at this later stage. To test this idea, we compared the number of cells in mitosis labeled by phosphohistone H3 (pH3) among CGNPs labeled by proliferating cell marker PCNA at E16.5. Analogous to E13.5, the proportion of $pH3^+$ cells among $PCNA^+$ cells in the EGL is unchanged despite the significantly reduced number of $pH3^+$ cells, suggesting that proliferation of CGNPs in the EGL is not compromised by the loss of Yap and Taz (Fig. 3M, Q, R). Additionally, to determine whether defects in cell survival play a role in the reduction of cerebellar size, we examined cell death at E13.5, when the reduction of URL becomes obvious, and at later stages, such as E15.5 and P7, by immunostaining for cleaved caspase (CC) 3. We found no obvious increase in cell death at these stages in the dCKO compared to WT control (Fig. S2), suggesting that cell death is not a major contributor to the reduced cerebellar size. Together, these results show that Yap/Taz loss reduces the size of URL but does not impair the proliferation of CGNPs in the EGL. Therefore, reduced production of cells in the stunted URL, which generates the initial pool of CGNPs in the EGL, may contribute to the decrease in cerebellar size.

Yap/Taz are not required for postnatal cerebellar granule cell progenitor proliferation

Yap is known to drive proliferation in various cellular contexts (Zhao et al., 2010) and over-expression of Yap drives proliferation of CGNPs in culture (Fernandez-L et al., 2009). Furthermore, Yap is often upregulated in several types of cancer (Johnson and Halder, 2013), including medulloblastoma, a tumor that arises in the cerebellum (Fernandez-L et al., 2009). As CGNPs extensively proliferate during postnatal stages, we sought to determine whether the loss of Yap/Taz in CGNPs affected their proliferative capacity during postnatal expansion stages. Through immunostaining and Western blot analyses, we are able to detect both Yap and Taz, which are substantially reduced at P0 in the *Nestin-Cre Taz* CKO, *Yap* heterozygote, and the dCKO (Fig. 4A, B). To confirm Cre recombination in EGL cells, we utilized a reporter mouse line ($ROSA^{mT/mG}$). Upon Cre recombination, membrane (m) GFP will be expressed instead of tdTomato due to Cre-mediated excision of the STOP signal in front of the GFP coding sequence (Muzumdar et al., 2007). At P3, GFP is expressed extensively throughout the cerebellum of the dCKO, including CGNPs, consistent with the absence of Yap expression (Fig. S3). To determine whether CGNPs without Yap/Taz exhibit proliferation defects, we counted $pH3^+$ cells in lobules II and III, where we detected consistent and unambiguous foliation defects (Fig. 4C). After $pH3^+$ cell numbers are normalized with lobe length, the number of $pH3^+$ cells in the dCKO is not significantly different from that in WT control (p=0.2228) (Fig. 4D). The proportion of $BrdU^+$ cells among total $Hoechst^+$ cells in the crown area of lobule III (100μm in length) is also similar to that of WT (p=0.3360) (Fig. 4E, F), evidence that CGNPs have no obvious proliferation defects in the absence of Yap and Taz during postnatal amplification. Next, as Shh produced

by PCs is the major mitogenic signal promoting postnatal CGNP amplification, we examined the effect of exogenous Shh on the proliferation of isolated dCKO CGNPs in culture. In contrast to shRNA-mediated knockdown experiments in which reduced Yap decreases the pro-proliferative effect of Shh (Fernandez-L et al., 2009), we failed to block Shh-mediated proliferation in CGNPs isolated from *Yap/Taz* dCKOs, despite greatly reduced Yap/Taz protein levels (Fig. 4G – I).

As our results differ from previous findings using shYap, we crossed $Yap^{f/f}/Taz^{f/f}$ mice to the *Math1-Cre* line, in which Cre is highly expressed in CGNPs (Yang et al., 2008), to further examine a potential cell autonomous effect of Yap/Taz loss on CGNP proliferation. We established efficient Yap/Taz removal by examining CGNPs in the oEGL at P0, when Yap expression in WT mice is evident. Yap expression in the CGNPs is notably absent in the CKO, while intense staining in the BG, choroid plexus, and meninges confirms reliable Yap detection (Fig. 5A). Western blot confirms the loss of Yap and shows a substantial reduction of Yap after granule cell isolation (Fig. 5B). Histological analyses demonstrated that the establishment of anchoring centers is not impaired, as the *Yap/Taz* dCKO cerebellum closely resembles that of WT at P0, P7, P14, and P21 (Fig. 5A, C, data not shown). Surprisingly, despite the lack of Yap/Taz, the proliferative capacity of CGNPs is not obviously affected, as determined by the same analyses done previously with *Nestin-Cre* animals (Fig. 4). There is a slight reduction of $pH3^+$ cells in lobules II and III, which does not reach statistical significance (Fig. 5D, E), and there are no changes in the proportion of $BrdU^+$ cells among total $Hoechst^+$ cells in the crown area of lobule III (Fig. 5F, G). To further confirm that the expression of Yap/Taz is diminished in the *Math1-Cre* dCKO animals during the postnatal amplification stage, we again utilized a reporter mouse line ($ROSA^{mT/mG}$). GFP is expressed in the EGL and IGL of the double mutant and almost completely overlaps with Pax6 immunostaining. The exception is in lobule X, where many $Pax6^+$ cells are not GFP^+, suggesting incomplete Cre recombination (Fig. 5H). The purity of granule cells and absence of Yap/Taz proteins are confirmed by lack of Yap immunostaining in GFP^+ Cre recombined granule cells, whereas tdTomato-expressing Cre^- granule cells show clear expression of Yap in culture (Fig. 5H, I). Together, Yap/Taz deletion from CGNPs in *Nestin-* or *Math1-Cre* transgenic mice does not produce significant proliferation defects, and Yap/Taz deletion by *Nestin-Cre* does not alter the CGNP response to Shh in culture.

Yap/Taz are not required for tumor initiation and progression in medulloblastoma arising from cells with constitutively active Smoothened

As the loss of Yap/Taz from CGNPs does not affect their proliferation during normal development, we designed the next set of experiments to determine the role of Yap in the pathogenesis of medulloblastoma. We utilized the well-established medulloblastoma model carrying the *SmoM2* allele, which expresses Smoothened, the downstream effector of Shh, with an activating mutation that is found in human medulloblastoma (W535L) (Mao et al., 2006). Conditionally expressing this allele under the control of *Math1-Cre* causes constitutively active Shh signaling in CGNPs and results in severe tumor formation. Despite previous studies demonstrating a function for Yap in pathogenesis of medulloblastoma arising from abnormal Shh signaling, knocking out *Yap* and *Taz* in this model did not reduce the severity of the SmoM2-induced tumor (Fig. 6A, B). As evidence, comparing the

proportion of tumor area, defined by high nuclear-cytoplasm ratio in H & E staining, among total cerebellum shows no difference between double heterozygote of Yap/Taz with SmoM2 allele (0.873, N=2) and dCKO with SmoM2 (0.872, N=5). Although it is possible that incomplete or escape from *Yap/Taz* loss may contribute to tumor persistence in the knockout mouse, confirmation of markedly reduced Yap expression in $Pax6^+$ cells at even later stages in the *SmoM2; Math1-Cre* mouse suggests that this is unlikely (Fig. 6C, C', D, D'). As Yap expression in glia is unchanged in the *Math1-Cre* model, Yap/Taz in glial cells may contribute to the tumor in the knockout mouse. Therefore, we examined Yap expression in the SmoM2 model using *hGFAP-Cre*, which eliminates Yap from glial cells as well as CGNPs. At P1, the absence of Yap is verified in the hypertrophic cerebellum of *Yap* and *SmoM2* double mutants, while its presence in endothelial, choroid plexus, and meningeal cells confirms reliable Yap staining (Fig. 6E, E', F, F'). Knocking out both *Yap* and *Taz* in the *SmoM2; hGFAP-Cre* mouse also does not appear to reduce the tumor size, as seen at P15 and older ages (data not shown). Although we cannot entirely rule out a role for Yap in medulloblastoma, it appears that Yap function is not required for the pathogenesis of Shh-mediated medulloblastoma resulting from constitutively active Smoothened in CGNPs. While we do not dispute that over-expression of Yap in CGNPs drives proliferation (Fernandez et al., 2009), our results suggest that the increased Yap expression observed in the proliferating CGNPs and Shh-mediated tumor cells of our transgenic mouse models is likely to be a consequence of proliferation signals rather than the cause.

Cerebellar radial glia scaffold formation requires Yap/Taz

To understand the function of Yap/Taz in cerebellar shape and foliation, we next looked for defects in neural progenitors in the VZ, where Yap expression is highly enriched (Fig. 1). The VZ generates subsets of deep cerebellar nuclei neurons and interneurons, PCs, and glia/interneuron progenitors, which propagate further in the white matter (Leto et al., 2016). At E13.5, Yap/Taz immunostaining is nearly undetectable in the dCKO while the cerebellar shape does not obviously differ from that of WT littermates. However, although $BLBP^+$ RGPs do not appear to be reduced in number, they are considerably dispersed in the dCKO, whereas they are tightly arranged in a few cell layers along the ventricular lining in the WT (Fig. 7A). It is evident that some of the $BLBP^+$ RGPs are displaced basally and some are maintained in the ventricular surface (Fig. 7A). We also assessed morphological deficits of RGPs in the dCKO by examining $BLBP^+$ cell shape and processes in later stages. At E15.5, the RGP cell bodies are abnormally elongated in a horizontal rather than vertical plane along the ventricular surface and also situated aberrantly in basal locations (Fig. 7B). Furthermore, in the dCKO, RGP processes are directed laterally instead of extending radially, which is a striking disruption of the radial scaffold (Fig 7B). Interestingly, at E16.5, the number of $BLBP^+$ RGPs in the dCKO is comparable to that of wild type despite the absence of $BLBP^+$ ventricular lining cells (Fig. 7C, D), suggesting that the major deficit is their abnormal shape and distribution rather than their production.

During and after embryogenesis, RGPs lose their apical processes, become BG, and translocate to the PCL (Buffo and Rossi, 2013), where they have a distinctive cell shape: their cell bodies are closely aligned with PCs and their radial processes extend to the pia. As Yap/Taz expression persists in BG during postnatal development and adult stages (Fig. 1F),

we carefully compared the position and morphology of BG in the dCKO and WT. At P0, more $BLBP^+$ BG cell bodies are found in the ML and EGL in the dCKO while BG cell bodies in the WT are mostly clustered at the PCL (Fig. 7E, S4). At P7, close examination of the fissures shows less organized BG cell bodies in the dCKO than in WT, when Yap expression remains absent in the BG of dCKO (Fig. 7F). At P10, severe foliation defects are readily seen in the dCKO (Fig. 7G), but most of the BG are properly localized to the PCL in both WT and dCKO then and thereafter (Fig S5). However, significantly fewer BG are found in lobules II and III of the dCKO (Fig. 7H). This is most likely due to the decreased length of these lobules because the density of BG, determined as the number of BG per 100μm, does not significantly differ between WT and dCKO (Fig. 7I). Furthermore, there is no significant difference between the numbers of BG associated with each PC in WT compared to dCKO (data not shown). Although we cannot definitively determine if the BG distribution defects and improper folia formation are related to each other or are independent consequences of Yap loss, the early improper BG positioning when secondary fissures form (Fig. 7E) may contribute to the defects. It is of note that the earlier distribution defects are corrected over time, suggesting that the maintenance of their location at the PCL does not require Yap/Taz. To test this, we used the *mGFAP-Cre* line to delete Yap/Taz from the glia population and examined later stages, such as P8, P21 and P90 months (Fig. S6). We confirmed that Cre recombined cells are mainly glia, including BG, as detected by the $ROSA^{mT/mG}$ reporter at P21. Cre recombined cells form a mosaic pattern, determined by GFP expression in the reporter mice, in which the expression of Yap is undetectable (Fig. S6). However, weak, distinct expression of Yap remains detectable in the GFP-negative area in lobule IX as well as in WT (data not shown and Fig. S5). Importantly, BG are not observed to be aberrantly located in the ML following glia-specific deletion of *Yap/Taz* at P21 and later stages such as P90 (Fig. S5). Thus, Yap/Taz are required for normal progression to establish the BG layer at the PCL but are not necessary to maintain proper BG position once established.

Yap/Taz are required for the junctional integrity of cerebellar neuroepithelium

As the most striking and consistent feature of Yap/Taz mutant is abnormal embryonic cerebellar shape associated with radial glia scaffold defects, we sought to further explore the causes of abnormal cell polarity and misdirected fiber phenotype. In the neuroepithelium, the apical junctional complex (AJC), comprising apical polarity complex proteins and adherens junction proteins, localizes at the apical endfeet of neural progenitors. The integrity of the AJC underlies the intact neuroepithelial architecture. Apical polarity complex proteins, such as Pals1 and Pard3, and adherens junction proteins, such as α−Catenin, are known to physically interact with Yap/Taz (Kohli et al., 2014; Schlegelmilch et al., 2011). Furthermore, their upstream regulators, such as NF2 (neurofibromatosis 2), KIBRA (kidney and brain expressed protein), and AMOT2 (Angiomotin 2), are known to be associated at the junction, highlighting the AJC as an important site of Yap/Taz regulation (Hirate et al., 2013; Meng et al., 2016). Recent studies also suggest an active role of Yap in junctional integrity and cytoskeletal protein regulation (Kim et al., 2017a; Neto et al., 2018). We therefore examined whether Yap/Taz-deficient RGPs fail to establish AJC. First, to determine whether apical polarity proteins are affected by the loss of Yap/Taz, we examined the localization of apical polarity complex proteins Pals1 (protein associated with Lin seven 1) and Crbs.

Apical polarity complex proteins are concentrated at the ventricular surface in the WT, whereas they are not localized at the ventricular surface at E13.5 in some areas of dCKO (Fig. 8A, B). At E16.5, apical complex proteins are absent in the entire lining of VZ in the *Yap/Taz* dCKO (Fig. 8E–H and data not shown). Similarly, adherens junction proteins N-Cadherin and β-Catenin are concentrated at the AJC in the WT, but are completely lacking in the dCKO by E16.5 and partially lost at E13.5 (Fig. 8A, B, E – H; data not shown). Because apical junctions are also maintained by actomyosin-mediated contractile force, we evaluated actomyosin integrity by Non-muscle Myosin IIB (NMIIB) distribution. NMIIB is no longer localized at the apical junction in the dCKO at E13.5 and E16.5, analogous to defects of other AJC components (Fig. 8C, D, I, J). To further confirm the loss of polarity and AJC in the absence of Yap/Taz, we used dCKO with *hGFAP-Cre* mice, which are known to have mosaic, delayed Cre expression at E12 and onward (Zhuo et al., 2001), compared to *Nestin-Cre*. At E14.5, Yap expression is partially lacking in the VZ of the dCKO, and Crb protein localization is reduced at the junctional areas where Yap expression is decreased (Fig. 8K, L). At E16.5, dCKO with *hGFAP-Cre* shows varying degrees of Yap/Taz loss and similar disruptions of the shape of $BLBP^{+}$ radial glia progenitors, junction proteins, and NMIIB distribution where Yap/Taz are lost (Fig. 8M – P, Fig. S7). As the disruption of junction protein localization correlates well with the loss of Yap/Taz, we further investigated whether their expression is altered in the Yap/Taz mutants. Since it is known that Yap/Taz promote the expression of NMIIB in other systems (Pavel et al., 2018), we examined the level of NMIIB and AJC components such as Pals1, N-Cadherin and β-Catenin in the cerebellum at E15.5. While Yap/Taz expression is substantially reduced, the levels of junction proteins are not altered in the *Yap/Taz* dCKO with *Nestin-Cre* (Fig. 8Q). Therefore, we concluded that expression levels of these junction complex proteins are not dependent on Yap/Taz, but rather that Yap/Taz are required for their proper localization at the junction. Together, Yap/Taz are necessary for the junctional integrity and cell polarity of RGP because they maintain AJC components at the junction. Interestingly, although it has been previously established that these junction proteins are also found in EGL cells and play a role in their proliferation and migration (Horn et al., 2018; Park et al., 2016a; Solecki, 2012; Trivedi et al., 2014), we did not observe any recognizable alterations in their distribution at P7 in the EGL of dCKOs (Fig. S8). Thus, the establishment of normal radial glia morphology requires Yap/Taz and the absence of critical Yap/Taz functions likely results in the abnormal cerebellar shape and potentially contributes to the aberrant secondary fissure formation during early postnatal stages.

DISCUSSION

Our study identifies a critical requirement for Yap/Taz in embryonic cerebellum morphogenesis and cellular features such as proliferation, shape, and polarity. Importantly, a small, flattened embryonic cerebellum is a consistent and significant feature of *Yap/Taz* double mutants, likely owing to disruption of the radial glia scaffold and proliferation defects. Because cerebellar size is already decreased at E15.5, before hydrocephalus develops in the dCKO; Nestin-Cre mice, the reduction observed during embryogenesis is unlikely to be due to the secondary consequences of elevated CSF pressure caused by hydrocephalus. Although we have not systematically compared the phenotypic penetrance of

Yap/Taz dCKO and Yap CKO, Yap-only CKO using Nestin-Cre can show the full spectrum of the cerebellar phenotype seen in the dCKO, including reduced cerebellar size, folia defects and hydrocephalus. Furthermore, following irradiation at early postnatal stages, Taz plays a minimal role in GC regeneration of Nestin^{+} progenitors in the PCL, whereas Yap makes a significant contribution to this process (Yang and Joyner, 2019). These observations suggest that Yap, but not Taz, has a major role in cerebellar development, consistent with its prominent expression in the developing cerebellum.

One of the most striking differences between WT and dCKO is a reduced number of cells in the stunted URL, although we are unable to distinguish whether the reduced size of URL is due to proliferation defects at an early stage (earlier than E13.5) or defects in regional specification of the URL. This observation suggests the critical need for Yap/Taz in the development and/or maintenance of this germinal zone and contrasts with our findings in both the embryonic and postnatal EGL, where proliferative capacity appears to be less dependent on Yap/Taz. The contrast highlights the differential requirements for Yap/Taz in cerebellar germinal zones. We do not have clear evidence of proliferation defects in VZ progenitors in the absence of Yap/Taz, as we did not detect a reduction of RGPs at E13.5 or E16.5. However, the number of PCs and BG, at least in lobules II and III, is decreased compared to WT at P10 (Fig. 7H). This reduction may indicate that early progenitors that generate PCs have proliferation or differentiation defects, although compromised PC survival cannot be completely ruled out. PCs generate the mitogenic signal Shh, which regulates not only CGNP proliferation but also BG production (Mecklenburg et al., 2014). Therefore, the reduced number of PCs found in *Yap/Taz* mutants may be responsible for the undersized cerebellum. Interestingly, it has been shown that progenitors that produce PCs have high E-Cadherin expression, which distinguishes them from interneuron progenitors (Mizuhara et al., 2010). Thus, it is possible that the specific proliferating zone affected by Yap/Taz loss may have a specialized junction protein composition. Further investigation will be necessary to establish Yap/Taz function in cerebellar progenitors in the VZ during early embryogenesis.

Our genetic study demonstrated that radial glia fibers are misdirected and polarized cellular architecture disrupted in the absence of Yap/Taz. This observation indicates that Yap/Taz play an important role in the establishment of the radial scaffold by RGPs in the embryonic cerebellum. A similar finding was reported in the Yap mutant of medaka fish, *hirame* (*hir*), in which deformation by gravity indicated the importance of Yap in tissue shaping (Porazinski et al., 2015). The flattened and misaligned 3D shape of *hir* mutants resulted from reduced actomyosin tension. In our study of the *Yap/Taz* deficient cerebellum, we found that the mutants lack a localized concentration of NMIIB at the apical junction (Fig 8D). Interestingly, the NMIIB mutant shows a hydrocephalus phenotype due to defects in ependymal cell generation, which is one of the major phenotypes of Yap loss in the brain (Park et al., 2016b). Despite *in vitro* studies consistently demonstrating that Yap/Taz are translocated to the nucleus in response to cues about tension mediated by actomyosin, the upstream role of Yap in actomyosin regulation is still emerging. For instance, recent studies reveal that Yap/Taz modulate upstream regulators of actomyosin activity, such as CDC42 and RhoA-ROCK. Since RhoA mutants show a similar small embryonic cerebellum, it is possible that Yap/Taz are required for proper RhoA-Rock regulation (Mulherkar et al.,

2014). This notion receives support from the finding that the *hir* Yap fish mutant lacks Yap-dependent expression of RhoA regulators such as the RhoGAP ArfGAP18 (Porazinski et al., 2015).

Alternatively, studies of the effects of disrupting apical polarity complex proteins at the junction have established that these proteins also play a role in actomyosin regulation and junctional integrity (Kishikawa et al., 2008; Roper, 2012). Although apical polarity complex proteins are known upstream regulators of Yap, our previous studies in the developing aqueduct are analogous to the present data in showing that disruption of apical polarity complex proteins and loss of AJ proteins at the apical junction immediately follow *Yap* knockdown (Park et al., 2016b). Interestingly, protein interaction profiling studies have identified some apical polarity complex proteins as Yap-interacting proteins (Kohli et al., 2014). Although it is unclear whether Yap/Taz can directly or indirectly interact with apical complex proteins in the cerebellar neuroepithelium, it is tempting to speculate that Yap/Taz are stabilizing the proteins at the junction through physical interactions with apical junction proteins such as Pals1 or Amotl2. An interaction between Crb3 and Yap/Taz has been found in alveolar epithelium, which contributes to inhibiting Yap/Taz nuclear translocation by promoting Lats1/2 mediated phosphorylation (Szymaniak et al., 2015). Thus, further investigation of interactions between Yap/Taz and polarity complex proteins and cytoskeletal regulators may reveal a new mechanism for Yap's role in establishing and/or maintaining junctional integrity in cerebellar neuroepithelium.

We also discovered an important Yap/Taz function in cerebellar folia development, especially the timely formation of secondary fissures. It is known that coordinated actions of PCs, CGNPs and BG are required for the proper commencement of fissure formation (Sudarov and Joyner, 2007). It has previously been demonstrated that CGNPs undergo reduced proliferation and cell shape changes at the fissure site. However, because *Math1-Cre* mediated deletion did not generate any obvious folia defects, we do not think that cell autonomous defects in cell shape change or proliferation are the likely cause of delayed fissure formation. One possibility is that a reduced number of CGNPs during embryogenesis impacted fissure formation due to an insufficient number of EGL cells. This notion receives support from our finding that the anterobasal lobe can be of variable size in dCKOs and that, when it is relatively large, there is a slight hint of a fissure, which appears as an indentation of the pia membrane and EGL layer. Furthermore, as precentral fissure formation was delayed but not absent, it is possible that a critical number of EGL cells may be required for proper fissure formation. Alternatively, early defects in the distribution of BG may underlie the delay in fissure formation, as correct BG fiber attachment to anchoring centers is known to be necessary to stabilize fissure bases (Sudarov and Joyner, 2007). Accordingly, BG development defects in multiple animal models including Ptpn11 mutants can cause folia defects (Leung and Li, 2018; Li et al., 2014). As BG distribution defects are corrected over time in the Yap/Taz dCKO, it is possible that the fissure base is stabilized when the distribution of BG around the fissure site is correctly positioned at the PCL in the *Yap/Taz* dCKO; *Nestin-Cre*. However, since dCKO; *hGFAP-Cre* mice rarely have folia defects, it is possible that scaffold defects of radial glia or BG distribution defects are not responsible for the folia defects. Nonetheless, we cannot rule out that widespread scaffold defects are required to cause folia defects as disrupted areas are variable in the *hGFAP-Cre* dCKO due

to the mosaic nature of Cre-expressing cells. Thus, future experiments that include using a glia-specific Cre expressed in BG, which sufficiently removes Yap/Taz from glia without affecting CGNPs, may clarify this issue.

By using various Cre drivers for targeted gene deletion, we have demonstrated that Yap/Taz function is critical for the initial placement of BG at the PC layer, but we were unable to establish a Yap/Taz function beyond the development of BG (Fig. S6). Interestingly, studies of the *Yap* mutant cerebral cortex have shown critical functions of Yap in glial cells and reported that Yap is required for the proliferation and differentiation of astrocytes through activation of BMP signaling (Huang et al., 2016). It has also been reported to play a significant role in Schwann cell proliferation and myelination by enhancing expression of Krox20, a transcription factor essential for the expression of genes critical for myelination (Grove et al., 2017; Lopez-Anido et al., 2016; Poitelon et al., 2016). However, in this study, we did not observe an active role of Yap in the cerebellum beyond early layer formation. Because Yap continues to be expressed in at least a subset of BG at later stages, it may have a persistent function in this cell type beyond development. Because of the well-established importance of Yap/Taz in regeneration, one such role may be in the response of BG to injury (Moya and Halder, 2018). Supporting this suggestion is the report that Müller glia, the scaffolding glia in the retina, also express Yap beyond development and that they increase its expression when photoreceptor cells undergo degeneration (Hamon et al., 2016). In early postnatal stages but not in adult, Yap function in Nestin^{+} progenitors residing in the PCL has been shown to be required for the survival and migration of regenerated CGNP/granule cells after irradiation, supporting a possible role in recovery from injury (Yang and Joyner, 2019). Thus, it is possible that Yap/Taz respond to injury signals and are involved in mediating cellular outcomes in CNS scaffolding glia such as BG and Müller glia.

Surprisingly, Yap/Taz loss from CGNPs does not alter proliferation during development or in SmoM2 tumors, even though Yap expression and stability are increased by Shh signaling and knockdown of *Yap* greatly reduces the proliferative response of cultured CGNPs to Shh (Fernandez et al., 2009). *Yap* is considered to act as an oncogene through its transcriptional activity and cooperation with Wnt signaling (Gregorieff et al., 2015; Kim et al., 2017b; Liu et al., 2018a), and Yap/Taz are amplified and transcriptionally active in several cancer types, including medulloblastoma, particularly in the SHH and WNT subgroups (Fernandez-L et al., 2009; Fernandez et al., 2009). In addition, its expression in tumor cells permits repopulation post-irradiation (Fernandez et al., 2012). Furthermore, a SHH:YAP:YB-1:IGF2 axis was recently identified in CGNPs, in which YB-1 increases IGF2 expression in a Yap-dependent manner (Dey et al., 2016). Importantly, YB-1 was found to be upregulated in human samples of all subtypes of medulloblastoma. This discrepancy suggests that transgenic *Yap/Taz* dCKO CGNPs, both *in vivo* and *in vitro*, may functionally compensate for Yap/Taz loss and respond to other mitogenic signals in ways that are not possible when Yap is knocked down acutely or deleted through Cre transfection in culture (Dey et al., 2016). Alternatively, it is also plausible that Yap is dispensable during initial tumor formation and development, and that it only becomes vital for tumor maintenance following irradiation through its proliferation-permissive role in cells with unrepaired DNA. If so, then Yap would be a potential therapeutic target in the specific context of radiotherapy

(Fernandez et al., 2012). Further investigation of the role of Yap in tumor establishment, progression, and recurrence is warranted.

In summary, our study shows for the first time that Yap/Taz are required for proper development of the cerebellar folia, and that they act primarily in radial glia and BG to promote proper placement and alignment of cells in the ventricular zone and PCL. The study also demonstrates that Yap is not required for CGNP proliferation during the postnatal expansion period although it is prominently expressed in these cells and we had highly anticipated an important role in promoting their cell cycle progression. Importantly, we have found that Yap/Taz are required for the establishment and maintenance of the AJC complex, which is necessary for junctional integrity and cell polarity.

Supplementary Material

Refer to Web version on PubMed Central for supplementary material.

Acknowledgements

We thank Dr. Tessler for editing our manuscript. We are grateful to Dr. Olson (Southwestern Medical School) who provided the Yap and Taz floxed mice. We appreciate Dr. Young-Gu Han (St. Jude Research Hospital) for critical inputs and sharing unpublished data. This work was supported by grants from the Shriners Hospitals for Children Research Grant (86100, 85109 to S.K.) and US National Institutes of Health (R01NS073112 to S.K). S. C. is supported by (R01EY020578).

REFERENCES

Buffo A, Rossi F, 2013 Origin, lineage and function of cerebellar glia. Prog Neurobiol 109, 42–63. [PubMed: 23981535]

Calvo F, Ege N, Grande-Garcia A, Hooper S, Jenkins RP, Chaudhry SI, Harrington K, Williamson P, Moeendarbary E, Charras G, Sahai E, 2013 Mechanotransduction and YAP-dependent matrix remodelling is required for the generation and maintenance of cancer-associated fibroblasts. Nature Cell Biology 15, 637–646. [PubMed: 23708000]

Cappello S, Gray MJ, Badouel C, Lange S, Einsiedler M, Srour M, Chitayat D, Hamdan FF, Jenkins ZA, Morgan T, Preitner N, Uster T, Thomas J, Shannon P, Morrison V, Di Donato N, Van Maldergem L, Neuhann T, Newbury-Ecob R, Swinkells M, Terhal P, Wilson LC, Zwijnenburg PJ, Sutherland-Smith AJ, Black MA, Markie D, Michaud JL, Simpson MA, Mansour S, McNeill H, Gotz M, Robertson SP, 2013 Mutations in genes encoding the cadherin receptor-ligand pair DCHS1 and FAT4 disrupt cerebral cortical development. Nat Genet 45, 1300–1308. [PubMed: 24056717]

Cho SH, Kim JY, Simons DL, Song JY, Le JH, Swindell EC, Jamrich M, Wu SM, Kim S, 2012 Genetic ablation of Pals1 in retinal progenitor cells models the retinal pathology of Leber congenital amaurosis. Hum Mol Genet 21, 2663–2676. [PubMed: 22398208]

Dey A, Robitaille M, Remke M, Maier C, Malhotra A, Gregorieff A, Wrana JL, Taylor MD, Angers S, Kenney AM, 2016 YB-1 is elevated in medulloblastoma and drives proliferation in Sonic hedgehog-dependent cerebellar granule neuron progenitor cells and medulloblastoma cells. Oncogene 35, 4256–4268. [PubMed: 26725322]

Dubois NC, Hofmann D, Kaloulis K, Bishop JM, Trumpp A, 2006 Nestin-Cre transgenic mouse line Nes-Cre1 mediates highly efficient Cre/loxP mediated recombination in the nervous system, kidney, and somite-derived tissues. Genesis 44, 355–360. [PubMed: 16847871]

Fernandez-L A, Northcott PA, Dalton J, Fraga C, Ellison D, Angers S, Taylor MD, Kenney AM, 2009 YAP1 is amplified and up-regulated in hedgehog-associated medulloblastomas and mediates Sonic hedgehog-driven neural precursor proliferation. Genes & Development 23, 2729–2741. [PubMed: 19952108]

Fernandez LA, Northcott PA, Dalton J, Fraga C, Ellison D, Angers S, Taylor MD, Kenney AM, 2009 YAP1 is amplified and up-regulated in hedgehog-associated medulloblastomas and mediates Sonic hedgehog-driven neural precursor proliferation. Genes Dev 23, 2729–2741. [PubMed: 19952108]

Fernandez LA, Squatrito M, Northcott P, Awan A, Holland EC, Taylor MD, Nahle Z, Kenney AM, 2012 Oncogenic YAP promotes radioresistance and genomic instability in medulloblastoma through IGF2-mediated Akt activation. Oncogene 31, 1923–1937. [PubMed: 21874045]

Gregorian C, Nakashima J, Le Belle J, Ohab J, Kim R, Liu A, Smith KB, Groszer M, Garcia AD, Sofroniew MV, Carmichael ST, Kornblum HI, Liu X, Wu H, 2009 Pten deletion in adult neural stem/progenitor cells enhances constitutive neurogenesis. J Neurosci 29, 1874–1886. [PubMed: 19211894]

Gregorieff A, Liu Y, Inanlou MR, Khomchuk Y, Wrana JL, 2015 Yap-dependent reprogramming of Lgr5(+) stem cells drives intestinal regeneration and cancer. Nature 526, 715–718. [PubMed: 26503053]

Grove M, Kim H, Santerre M, Krupka AJ, Han SB, Zhai J, Cho JY, Park R, Harris M, Kim S, Sawaya BE, Kang SH, Barbe MF, Cho SH, Lemay MA, Son YJ, 2017 YAP/TAZ initiate and maintain Schwann cell myelination. Elife 6.

Halder G, Dupont S, Piccolo S, 2012 Transduction of mechanical and cytoskeletal cues by YAP and TAZ. Nat Rev Mol Cell Biol 13, 591–600. [PubMed: 22895435]

Hamon A, Roger JE, Yang XJ, Perron M, 2016 Muller glial cell-dependent regeneration of the neural retina: An overview across vertebrate model systems. Dev Dyn 245, 727–738. [PubMed: 26661417]

Hao J, Zhang Y, Wang Y, Ye R, Qiu J, Zhao Z, Li J, 2014 Role of extracellular matrix and YAP/TAZ in cell fate determination. Cell Signal 26, 186–191. [PubMed: 24216612]

Harvey KF, Hariharan IK, 2012 The hippo pathway. Cold Spring Harb Perspect Biol 4, a011288. [PubMed: 22745287]

Hirate Y, Hirahara S, Inoue K, Suzuki A, Alarcon VB, Akimoto K, Hirai T, Hara T, Adachi M, Chida K, Ohno S, Marikawa Y, Nakao K, Shimono A, Sasaki H, 2013 Polarity-dependent distribution of angiomotin localizes Hippo signaling in preimplantation embryos. Curr Biol 23, 1181–1194. [PubMed: 23791731]

Hong W, Guan KL, 2012 The YAP and TAZ transcription co-activators: key downstream effectors of the mammalian Hippo pathway. Semin Cell Dev Biol 23, 785–793. [PubMed: 22659496]

Horn Z, Behesti H, Hatten ME, 2018 N-cadherin provides a cis and trans ligand for astrotactin that functions in glial-guided neuronal migration. Proc Natl Acad Sci U S A 115, 10556–10563. [PubMed: 30262652]

Huang Z, Hu J, Pan J, Wang Y, Hu G, Zhou J, Mei L, Xiong WC, 2016 YAP stabilizes SMAD1 and promotes BMP2-induced neocortical astrocytic differentiation. Development 143, 2398–2409. [PubMed: 27381227]

Johnson R, Halder G, 2013 The two faces of Hippo: targeting the Hippo pathway for regenerative medicine and cancer treatment. Nature Reviews Drug Discovery 13, 63–79. [PubMed: 24336504]

Johnson R, Halder G, 2014 The two faces of Hippo: targeting the Hippo pathway for regenerative medicine and cancer treatment. Nat Rev Drug Discov 13, 63–79. [PubMed: 24336504]

Kim J, Kim YH, Kim J, Park DY, Bae H, Lee DH, Kim KH, Hong SP, Jang SP, Kubota Y, Kwon YG, Lim DS, Koh GY, 2017a YAP/TAZ regulates sprouting angiogenesis and vascular barrier maturation. J Clin Invest 127, 3441–3461. [PubMed: 28805663]

Kim JY, Park R, Lee JH, Shin J, Nickas J, Kim S, Cho SH, 2016 Yap is essential for retinal progenitor cell cycle progression and RPE cell fate acquisition in the developing mouse eye. Dev Biol 419, 336–347. [PubMed: 27616714]

Kim W, Khan SK, Gvozdenovic-Jeremic J, Kim Y, Dahlman J, Kim H, Park O, Ishitani T, Jho EH, Gao B, Yang Y, 2017b Hippo signaling interactions with Wnt/beta-catenin and Notch signaling repress liver tumorigenesis. J Clin Invest 127, 137–152. [PubMed: 27869648]

Kishikawa M, Suzuki A, Ohno S, 2008 aPKC enables development of zonula adherens by antagonizing centripetal contraction of the circumferential actomyosin cables. J Cell Sci 121, 2481–2492. [PubMed: 18628308]

Kohli P, Bartram MP, Habbig S, Pahmeyer C, Lamkemeyer T, Benzing T, Schermer B, Rinschen MM, 2014 Label-free quantitative proteomic analysis of the YAP/TAZ interactome. Am J Physiol Cell Physiol 306, C805–818. [PubMed: 24573087]

Lee HY, Greene LA, Mason CA, Manzini MC, 2009 Isolation and culture of post-natal mouse cerebellar granule neuron progenitor cells and neurons. J Vis Exp.

Leto K, Arancillo M, Becker EB, Buffo A, Chiang C, Ding B, Dobyns WB, Dusart I, Haldipur P, Hatten ME, Hoshino M, Joyner AL, Kano M, Kilpatrick DL, Koibuchi N, Marino S, Martinez S, Millen KJ, Millner TO, Miyata T, Parmigiani E, Schilling K, Sekerkova G, Sillitoe RV, Sotelo C, Uesaka N, Wefers A, Wingate RJ, Hawkes R, 2016 Consensus Paper: Cerebellar Development. Cerebellum 15, 789–828. [PubMed: 26439486]

Leung AW, Li JYH, 2018 The Molecular Pathway Regulating Bergmann Glia and Folia Generation in the Cerebellum. Cerebellum 17, 42–48. [PubMed: 29218544]

Li K, Leung AW, Guo Q, Yang W, Li JY, 2014 Shp2-dependent ERK signaling is essential for induction of Bergmann glia and foliation of the cerebellum. J Neurosci 34, 922–931. [PubMed: 24431450]

Liu H, Du S, Lei T, Wang H, He X, Tong R, Wang Y, 2018a Multifaceted regulation and functions of YAP/TAZ in tumors (Review). Oncol Rep 40, 16–28. [PubMed: 29749524]

Liu WA, Chen S, Li Z, Lee CH, Mirzaa G, Dobyns WB, Ross ME, Zhang J, Shi SH, 2018b PARD3 dysfunction in conjunction with dynamic HIPPO signaling drives cortical enlargement with massive heterotopia. Genes Dev 32, 763–780. [PubMed: 29899142]

Lopez-Anido C, Poitelon Y, Gopinath C, Moran JJ, Ma KH, Law WD, Antonellis A, Feltri ML, Svaren J, 2016 Tead1 regulates the expression of Peripheral Myelin Protein 22 during Schwann cell development. Hum Mol Genet 25, 3055–3069. [PubMed: 27288457]

Mao J, Ligon KL, Rakhlin EY, Thayer SP, Bronson RT, Rowitch D, McMahon AP, 2006 A novel somatic mouse model to survey tumorigenic potential applied to the Hedgehog pathway. Cancer Res 66, 10171–10178. [PubMed: 17047082]

Matei V, Pauley S, Kaing S, Rowitch D, Beisel KW, Morris K, Feng F, Jones K, Lee J, Fritzsch B, 2005 Smaller inner ear sensory epithelia in Neurog 1 null mice are related to earlier hair cell cycle exit. Dev Dyn 234, 633–650. [PubMed: 16145671]

Mecklenburg N, Martinez-Lopez JE, Moreno-Bravo JA, Perez-Balaguer A, Puelles E, Martinez S, 2014 Growth and differentiation factor 10 (Gdf10) is involved in Bergmann glial cell development under Shh regulation. Glia 62, 1713–1723. [PubMed: 24963847]

Meng Z, Moroishi T, Guan KL, 2016 Mechanisms of Hippo pathway regulation. Genes Dev 30, 1–17. [PubMed: 26728553]

Mizuhara E, Minaki Y, Nakatani T, Kumai M, Inoue T, Muguruma K, Sasai Y, Ono Y, 2010 Purkinje cells originate from cerebellar ventricular zone progenitors positive for Neph3 and E-cadherin. Dev Biol 338, 202–214. [PubMed: 20004188]

Moon S, Yeon Park S, Woo Park H, 2018 Regulation of the Hippo pathway in cancer biology. Cell Mol Life Sci 75, 2303–2319. [PubMed: 29602952]

Moya IM, Halder G, 2018 Hippo-YAP/TAZ signalling in organ regeneration and regenerative medicine. Nat Rev Mol Cell Biol.

Mulherkar S, Uddin MD, Couvillon AD, Sillitoe RV, Tolias KF, 2014 The small GTPases RhoA and Rac1 regulate cerebellar development by controlling cell morphogenesis, migration and foliation. Dev Biol 394, 39–53. [PubMed: 25128586]

Muzumdar MD, Tasic B, Miyamichi K, Li L, Luo L, 2007 A global double-fluorescent Cre reporter mouse. Genesis 45, 593–605. [PubMed: 17868096]

Neto F, Klaus-Bergmann A, Ong YT, Alt S, Vion AC, Szymborska A, Carvalho JR, Hollfinger I, Bartels-Klein E, Franco CA, Potente M, Gerhardt H, 2018 YAP and TAZ regulate adherens junction dynamics and endothelial cell distribution during vascular development. Elife 7.

Orr BA, Bai H, Odia Y, Jain D, Anders RA, Eberhart CG, 2011 Yes-associated protein 1 is widely expressed in human brain tumors and promotes glioblastoma growth. J Neuropathol Exp Neurol 70, 568–577. [PubMed: 21666501]

Park JY, Hughes LJ, Moon UY, Park R, Kim SB, Tran K, Lee JS, Cho SH, Kim S, 2016a The apical complex protein Pals1 is required to maintain cerebellar progenitor cells in a proliferative state. Development 143, 133–146. [PubMed: 26657772]

Park R, Moon UY, Park JY, Hughes LJ, Johnson RL, Cho SH, Kim S, 2016b Yap is required for ependymal integrity and is suppressed in LPA-induced hydrocephalus. Nat Commun 7, 10329. [PubMed: 26754915]

Pavel M, Renna M, Park SJ, Menzies FM, Ricketts T, Fullgrabe J, Ashkenazi A, Frake RA, Lombarte AC, Bento CF, Franze K, Rubinsztein DC, 2018 Contact inhibition controls cell survival and proliferation via YAP/TAZ-autophagy axis. Nat Commun 9, 2961. [PubMed: 30054475]

Poitelon Y, Lopez-Anido C, Catignas K, Berti C, Palmisano M, Williamson C, Ameroso D, Abiko K, Hwang Y, Gregorieff A, Wrana JL, Asmani M, Zhao R, Sim FJ, Wrabetz L, Svaren J, Feltri ML, 2016 YAP and TAZ control peripheral myelination and the expression of laminin receptors in Schwann cells. Nat Neurosci 19, 879–887. [PubMed: 27273766]

Porazinski S, Wang H, Asaoka Y, Behrndt M, Miyamoto T, Morita H, Hata S, Sasaki T, Krens SFG, Osada Y, Asaka S, Momoi A, Linton S, Miesfeld JB, Link BA, Senga T, Shimizu N, Nagase H, Matsuura S, Bagby S, Kondoh H, Nishina H, Heisenberg CP, Furutani-Seiki M, 2015 YAP is essential for tissue tension to ensure vertebrate 3D body shape. Nature 521, 217–221. [PubMed: 25778702]

Roper K, 2012 Anisotropy of Crumbs and aPKC drives myosin cable assembly during tube formation. Dev Cell 23, 939–953. [PubMed: 23153493]

Roussel MF, Hatten ME, 2011 Cerebellum development and medulloblastoma. Curr Top Dev Biol 94, 235–282. [PubMed: 21295689]

Schlegelmilch K, Mohseni M, Kirak O, Pruszak J, Rodriguez JR, Zhou D, Kreger BT, Vasioukhin V, Avruch J, Brummelkamp TR, Camargo FD, 2011 Yap1 acts downstream of alpha-catenin to control epidermal proliferation. Cell 144, 782–795. [PubMed: 21376238]

Solecki DJ, 2012 Sticky situations: recent advances in control of cell adhesion during neuronal migration. Curr Opin Neurobiol 22, 791–798. [PubMed: 22560352]

Song JY, Park R, Kim JY, Hughes L, Lu L, Kim S, Johnson RL, Cho SH, 2014 Dual function of Yap in the regulation of lens progenitor cells and cellular polarity. Dev Biol 386, 281–290. [PubMed: 24384391]

Sudarov A, Joyner AL, 2007 Cerebellum morphogenesis: the foliation pattern is orchestrated by multi-cellular anchoring centers. Neural Dev 2, 26. [PubMed: 18053187]

Szymaniak AD, Mahoney JE, Cardoso WV, Varelas X, 2015 Crumbs3-Mediated Polarity Directs Airway Epithelial Cell Fate through the Hippo Pathway Effector Yap. Dev Cell 34, 283–296. [PubMed: 26235047]

Trivedi N, Ramahi JS, Karakaya M, Howell D, Kerekes RA, Solecki DJ, 2014 Leading-process actomyosin coordinates organelle positioning and adhesion receptor dynamics in radially migrating cerebellar granule neurons. Neural Dev 9, 26. [PubMed: 25467954]

Varelas X, 2014 The Hippo pathway effectors TAZ and YAP in development, homeostasis and disease. Development 141, 1614–1626. [PubMed: 24715453]

Xin M, Kim Y, Sutherland LB, Murakami M, Qi X, McAnally J, Porrello ER, Mahmoud AI, Tan W, Shelton JM, Richardson JA, Sadek HA, Bassel-Duby R, Olson EN, 2013 Hippo pathway effector Yap promotes cardiac regeneration. Proc Natl Acad Sci U S A 110, 13839–13844. [PubMed: 23918388]

Yang Z-J, Ellis T, Markant SL, Read T-A, Kessler JD, Bourboulas M, Schüller U, Machold R, Fishell G, Rowitch DH, Wainwright BJ, Wechsler-Reya RJ, 2008 Medulloblastoma Can Be Initiated by Deletion of Patched in Lineage-Restricted Progenitors or Stem Cells. Cancer Cell 14, 135–145. [PubMed: 18691548]

Yang Z, Joyner AL, 2019 YAP1 is involved in replenishment of granule cell precursors following injury to the neonatal cerebellum. Dev Biol.

Yu FX, Zhao B, Panupinthu N, Jewell JL, Lian I, Wang LH, Zhao J, Yuan H, Tumaneng K, Li H, Fu XD, Mills GB, Guan KL, 2012 Regulation of the Hippo-YAP pathway by G-protein-coupled receptor signaling. Cell 150, 780–791. [PubMed: 22863277]

Zhao B, Li L, Lei Q, Guan KL, 2010 The Hippo-YAP pathway in organ size control and tumorigenesis: an updated version. Genes Dev 24, 862–874. [PubMed: 20439427]

Zhuo L, Theis M, Alvarez-Maya I, Brenner M, Willecke K, Messing A, 2001 hGFAP-cre transgenic mice for manipulation of glial and neuronal function in vivo. Genesis 31, 85–94. [PubMed: 11668683]

1. Yap/Taz are required for cerebellar morphogenesis by establishing the radial glia scaffold and cellular polarity.
2. Yap/Taz deletion causes abnormal folia development due to defects in secondary fissure formation.
3. Yap/Taz are dispensable for the proliferation of cerebellar granule neuron precursors and of medulloblastoma tumor cells caused by constitutively active Smoothened.
4. Yap/Taz are necessary to establish and maintain junctional integrity of the cerebellar neuroepithelium.

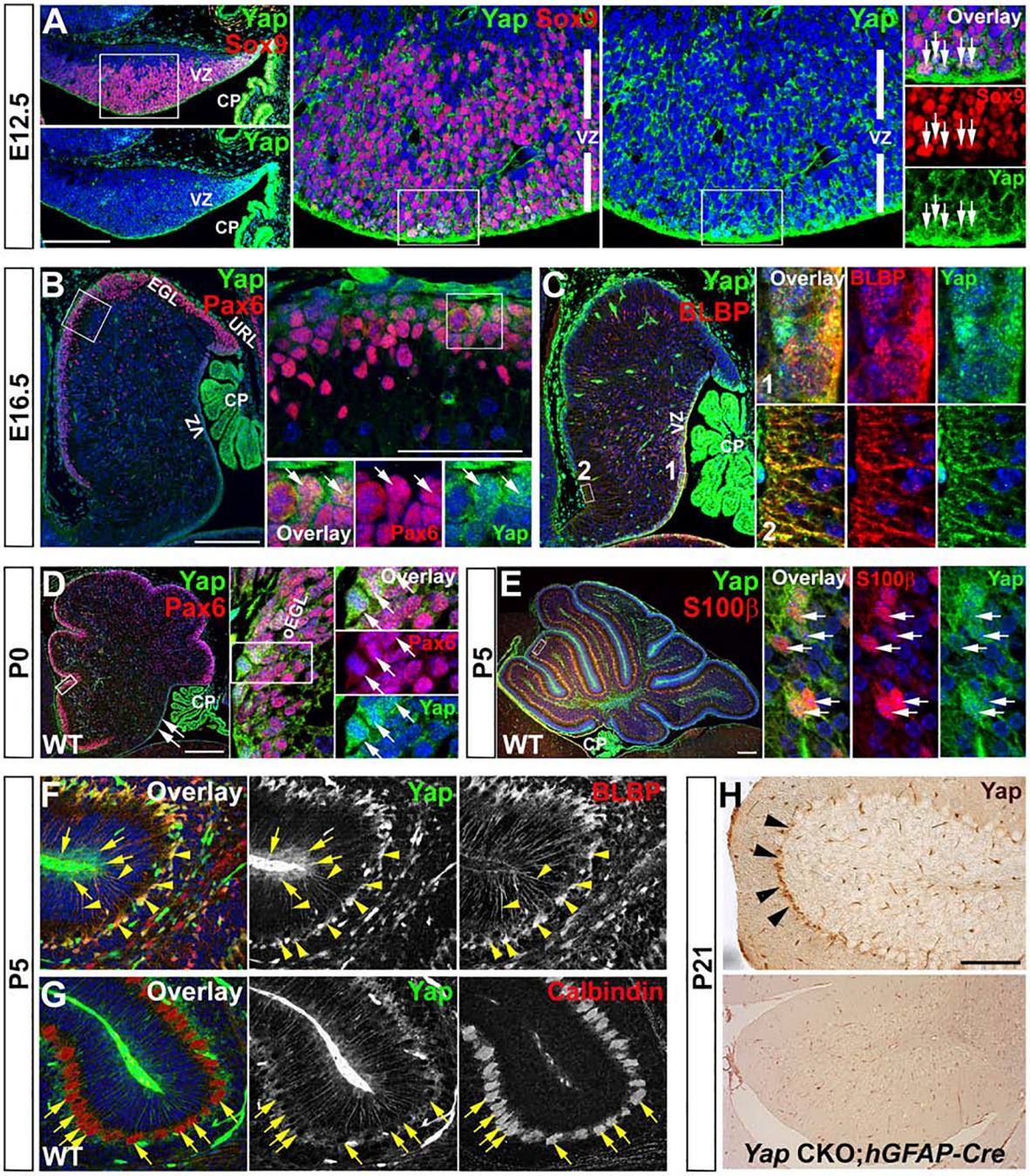

Figure 1. Yap expression is temporally and spatially dynamic in the developing cerebellum.

(**A**) Yap is highly expressed in proliferating zones labeled with Sox9 in the E12.5 cerebellum (arrows). (**B,C**) Yap expression remains high in the EGL (arrows, marked with Pax6), VZ cells (marked by BLBP) at E16.5. (**D**) At P0, Yap is enriched in $Pax6^{+}$ cells in the oEGL. (**E**) Yap expression overlaps with $S100\beta^{+}$ BG in the nucleus (arrows) at P5. (**F,G**) Yap and BLBP double staining shows strong Yap expression in GNPs in the oEGL (arrows) and in the soma and processes of the $BLBP^{+}$ BG (arrowheads) while double staining with Calbindin shows Yap is not detectable in PCs. (**H**) In adult mice, Yap expression persists in

at least a subset of BG (arrowheads) and Yap is not detected in BG of CKO mice (arrowheads, *Yap* CKO; *hGFAP-Cre*). VZ: ventricular zone, URL: upper rhombic lip, oEGL: outer external granular layer, CP: Choroid Plexus, BG: Bergmann glia.

*Scale bars: Low magnification images: 200μm. Enlarged high magnification images: 50μm.

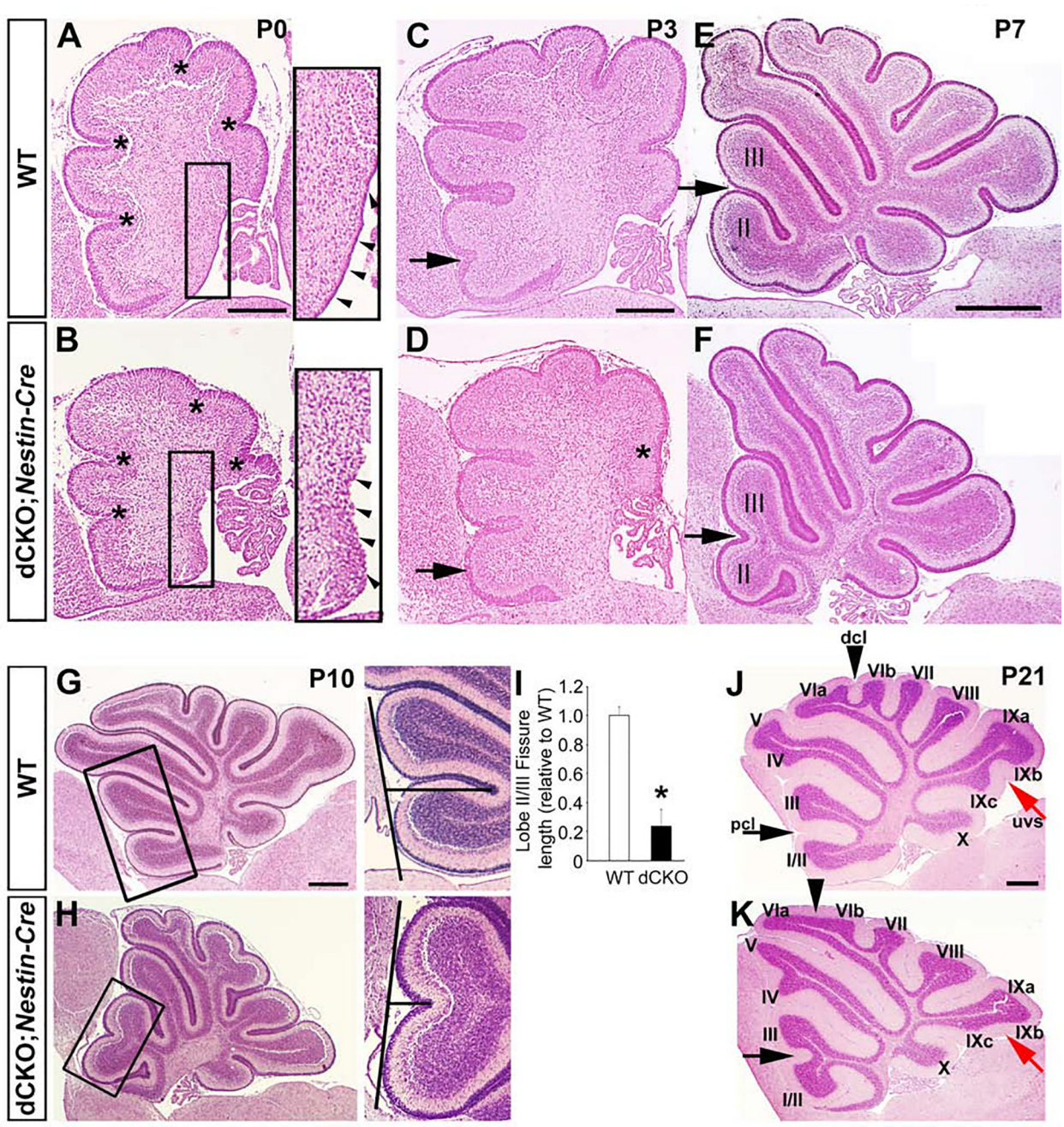

Figure 2. Yap/Taz are required for proper foliation.

(A, B) At P0, the four principal fissures are apparent in both the WT and the *Yap/Taz* dCKO; *Nestin-Cre* (asterisks), but the ventricular lining is notably missing in the dCKO (inset). (**C**, **D)** Secondary fissures between lobules II and III are formed at P3 in the WT but not in the dCKOs (arrows). Asterisk shows less distinct posterolateral principal fissure in dCKO **(D)**. **(E, F)** Foliation defects are pronounced in P7 dCKO mice compared to WT, with the most consistently observed defect being the incomplete non-principal fissure formation between lobules II and III (arrows). (**G**, **H**) WT precentral fissure is prominent at P10 while precentral fissure in the dCKO is notably shorter. Precentral fissure length was defined by

the length of a line from the base of the fissure perpendicular to a line tangential to the crowns of lobules II and III in the WT and dCKO (**G** and **H**, respectively). (**I**) Statistical analysis of precentral fissure length revealed a significantly shorter fissure in dCKO mice compared to WT at P10 ($p = 2.5\times10^{-13}$). (**J**) P21 WT cerebellum exhibits a characteristic foliation pattern. (**K**) dCKOs have foliation defects, particularly at the precentral fissure (pcl) between lobules II and III. No clear separation between VIa and VIb (dcl, declival sulcus, arrow heads) is found and lobe IX is underdeveloped with no apparent uvs (uvular sulcus, red arrow). All histological images are representative of at least three animals for each genotype and stage.

*Scale bars: P0, P3: 250μm; P7, P10, P21: 500μm.

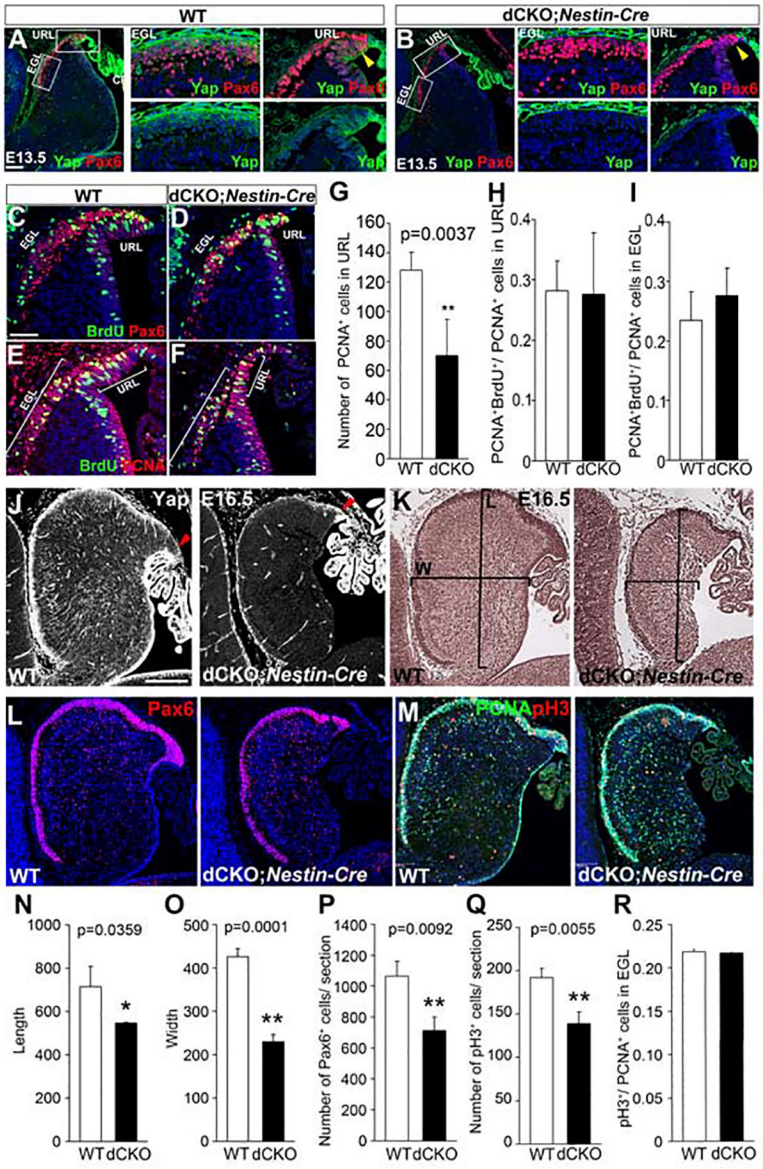

Figure 3. Yap/Taz loss causes hypoplastic slender cerebellum

(A, B) At E13.5, Yap expression is found in all three germ layers, including the Pax6^{+} EGL and URL, but is no longer seen in the *Yap/Taz* dCKO; *Nestin-Cre.* Although cerebellar size in the dCKO is unchanged, the URL is notably smaller than that of WT (arrowheads). **(C-F)** URL cells are PCNA+ and the majority of Pax6+ cells in the EGL are proliferating cells marked by PCNA. (URL and EGL are indicated by brackets in the **E** and **F**). **(G)** The number of PCNA^{+} proliferating cells in the URL is reduced in the dCKO (N=5) compared to WT (N=4) **(H-I)** The proportion of BrdU labeled S-phase cells among total PCNA^{+} cells is determined in the URL **(H)** and EGL **(I)** and compared between WT (N=4) and dCKO (N=5). (**J)** At E16.5, Yap expression in the dCKO is **l**argely undetectable and URL size reduced. **(K, N, O)** Both width **(N)** and length **(O)** of the cerebellum are strikingly reduced in the dCKO compared to WT (N=3, WT and *Nestin-Cre* dCKO). **(L, P)** Total number of Pax6^{+} cells in CGNP/CGN and URL is strikingly reduced in the dCKO compared to WT

(N=3, WT and *Nestin-Cre* dCKO). **(M, Q, R)** Cells in mitosis, labeled by pH3 immunostaining, are reduced in number in the dCKO **(M, Q)** but the proportion of $pH3^+$ cells among total PCNA+ proliferating cells in the EGL is not significantly different from WT (N=3, WT and *Nestin-Cre* dCKO) (**R).**

*Scale bar: 100μm

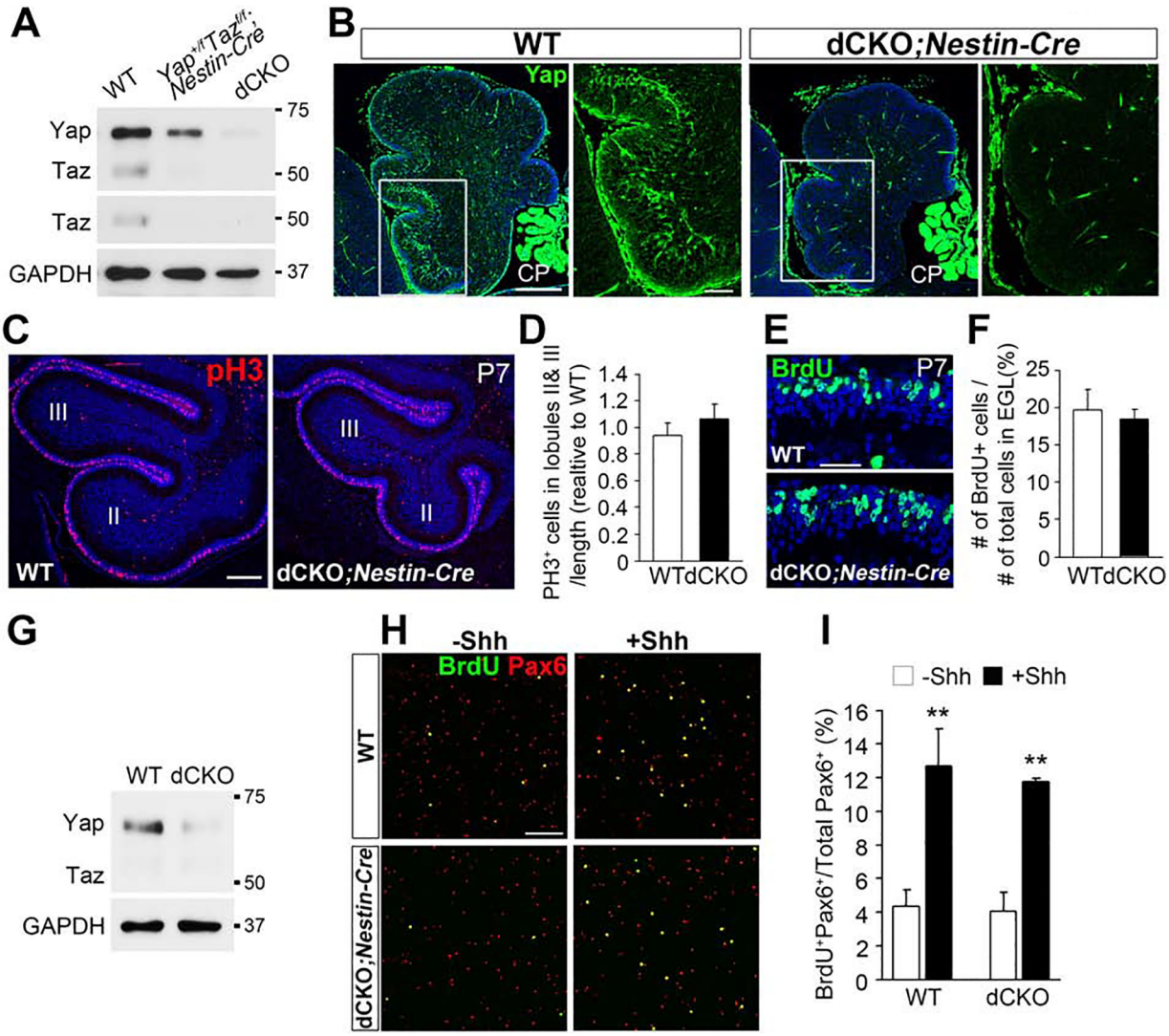

Figure 4. *Yap/Taz* deletion by *Nestin-Cre* does not alter CGNP proliferation or Shh response in culture.

(A) Western blot of whole cerebellum from P0 animals from WT, *Yap*$^{f/+}$*Taz*$^{f/f}$;*Nestin-Cre* and dCKO;*Nestin-Cre* shows relative abundance of Yap and Taz in WT and efficient reduction of both proteins in the mutants (N=3, WT; N=2, *Yap*$^{f/+}$*Taz*$^{f/f}$;*Nestin-Cre*; N=3, dCKO). **(B)** In the dCKO, Yap is undetectable in the EGL and BG at P0 (N=3, WT and *Nestin-Cre* dCKO). **(C, D)** Mitotic pH3^{+} cells in lobules II and III are not reduced in number when normalized with lobe length in the dCKO; *Nestin-Cre* (p=0.2228). **(E, F)** The fraction of BrdU^{+} S-phase cells among total Hoechst^{+} EGL cells is not significantly different in dCKO compared to WT (p=0.3360). **(G)** Taz is undetectable in both WT and dCKO cerebellar granule cells after percoll gradient separation and Yap is nearly undetectable in the dCKO (N=2, WT and N=2, dCKO;*Nestin-Cre*). **(H, I)** In cerebellar granule cell culture, Shh treatment increases the mitogenic response, shown by increased BrdU^{+} S-phase cells (green) among Pax6^{+} cells (red), in both WT (N=3, Shh treatment, p=0.03939) and dCKO cells (N=3, Shh treatment p=0.00035), with no difference in Shh response between WT and dCKO CGNPs (WT +Shh vs. dCKO +Shh, p=0.506).

*Scale bars: **B** low magnification, **C**:150 μm; **B** high magnification, **E**: 50 μm; **H**: 100 μm.

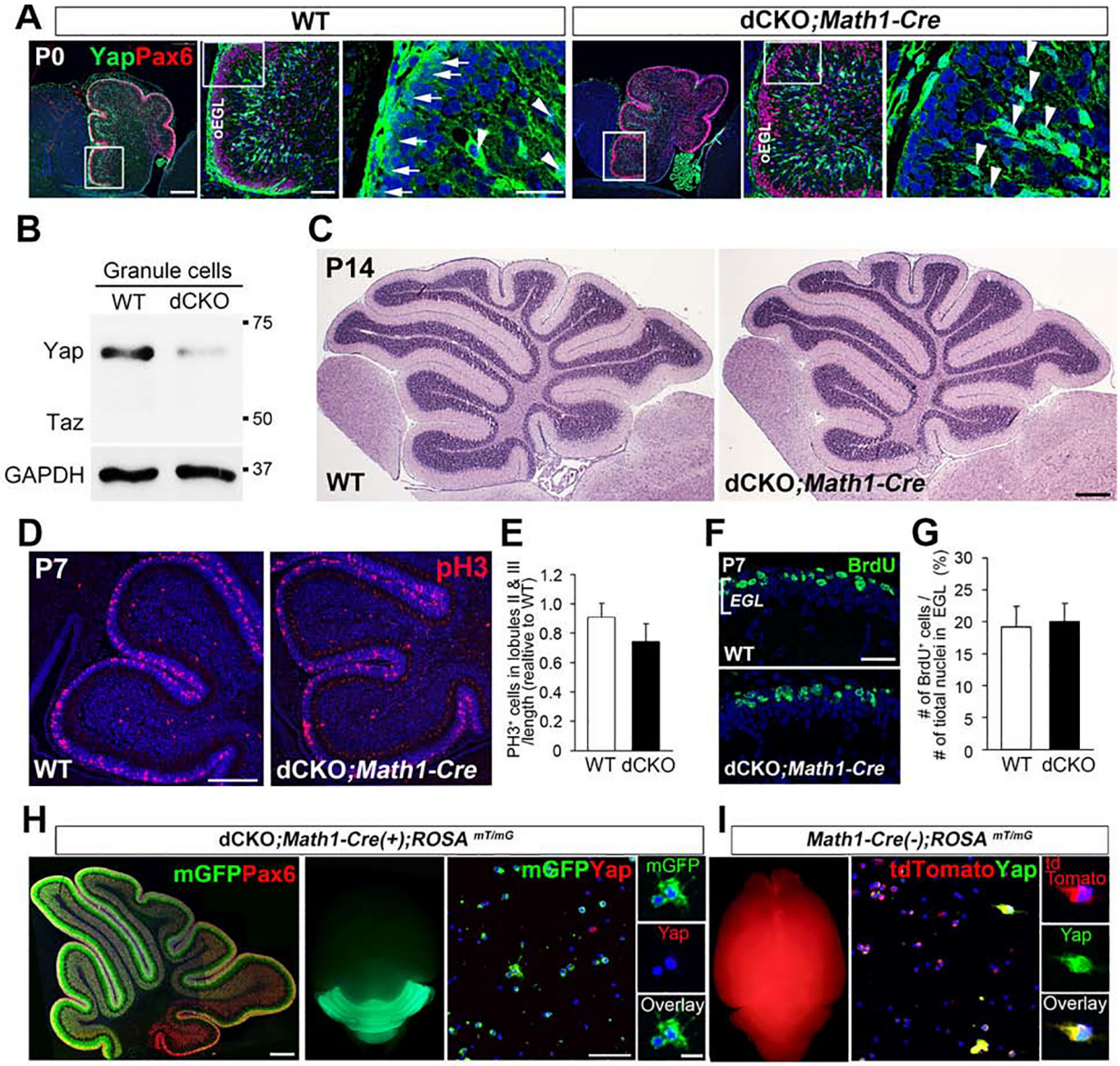

Figure 5. *Yap/Taz* deletion by *Math1-Cre* does not alter CGNP proliferation.

(**A**) At P0, Yap expression in WT can be detected in the nuclei of cells in the oEGL (arrows), where proliferating Pax6^{+} CGNPs are located, as well as in BG (arrowheads). Loss of Yap in the oEGL is observed in the dCKO;*Math1-Cre* while it remains in BG (arrowheads), meninges and choroid plexus. **(B)** Taz is nearly undetectable in both WT and dCKO;*Math1-Cre* cerebellar granule cells after percoll gradient separation and Yap is substantially reduced in the dCKO compared to WT (N=2, WT; N=2, dCKO). (**C**) *Yap/Taz* deletion from CGNPs does not noticeably affect cerebellar development by P14. **(D, E)** The number of pH3^{+} mitotic cells in lobules II and III is not significantly different when normalized with lobe length in the dCKO; *Math1-Cre* (p=0.1367). **(F, G)** The proportion of BrdU^{+} S-phase cells in total EGL cells (Hoechst^{+}) is similar in WT and dCKO;*Math1-Cre* (p=0.625). **(H-I)** mGFP expression, indicating Cre recombination, is evident in CGNPs and granule neurons in cerebellar lobes, except lobe X, at P7 in the dCKO using the ROSA$^{mT/mG}$ reporter line

(N=2, dCKO). Whole brain images show ubiquitous tdTomato expression in unrecombined cells, while mGFP expression is specifically restricted to the cerebellum in the ROSA$^{mT/mG}$;*Math1-Cre* mouse. Cerebellar granule cell culture from dCKO;*Math1-Cre* shows mGFP expressing cells lack Yap expression, whereas Cre^{-} WT granule cells expressing tdTomato show Yap expression (N=2, WT; N=2 dCKO;*Math1-Cre*).
*Scale bars: **A** low magnification, **C, D**: 150 μm; **A** high magnifications, **H, I:** 50 μm, **C**, **H** low magnification: 200 μm, **F**: 25μm; **H, I insets**: 10 μm.

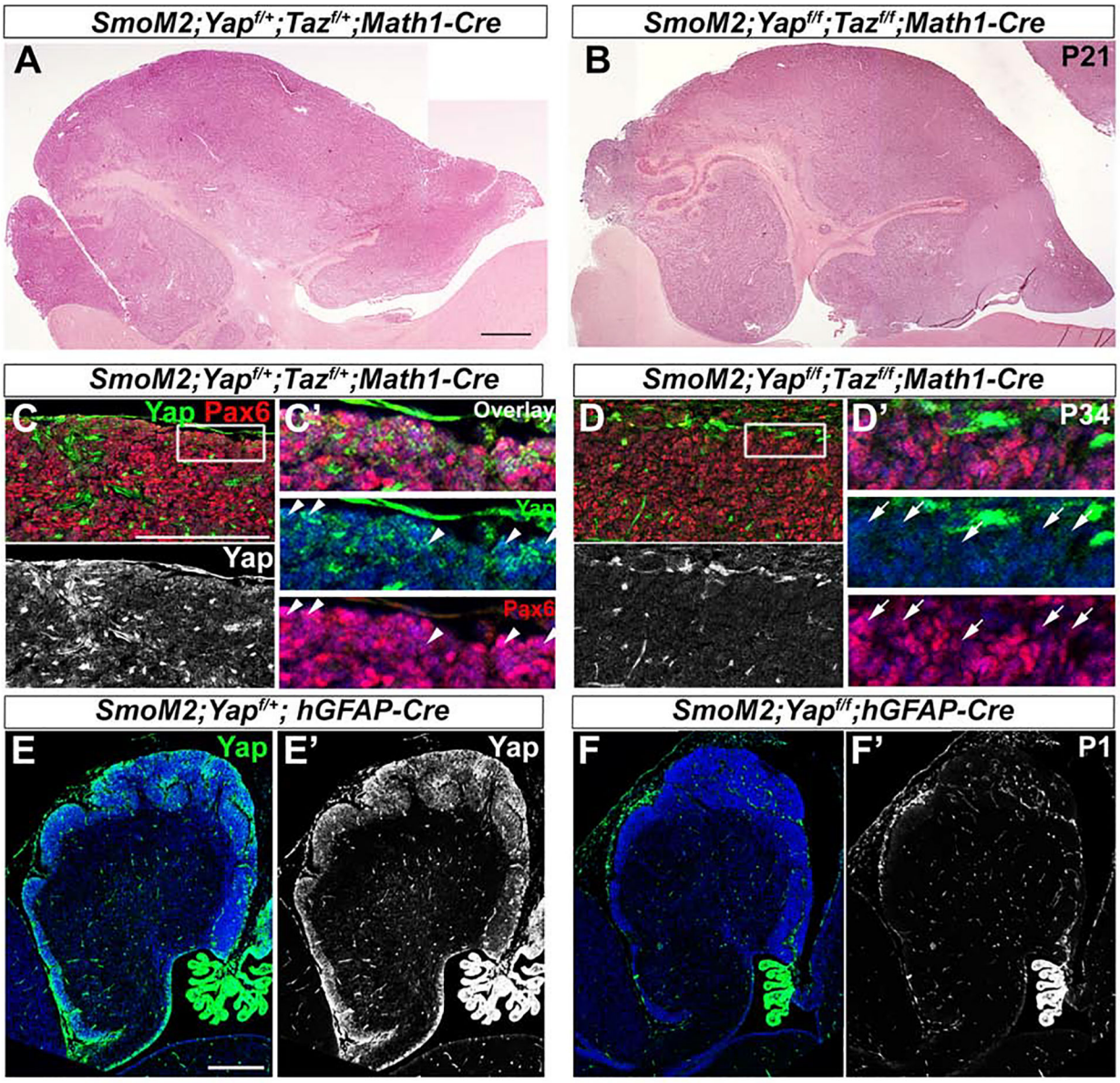

Figure 6. Yap/Taz do not mediate overproliferation induced by constitutively active Smo.

(**A**) Constitutively active Shh signaling (SmoM2) in CGNPs results in a huge tumor burden at P21, which is not relieved by (**B**) Yap/Taz loss. (**C, C'**) Yap expression is ubiquitously observed in Pax6^{+} cells of the *Math1-Cre* driven SmoM2 tumor (arrowheads) but (**D**, **D'**) is markedly reduced in the *SmoM2*; *Yap* $^{f/f}$; *Taz* $^{f/f}$; *Math1-Cre* tumor (arrows, N=3, *SmoM2*; *Yap*$^{f/+}$; *Taz*$^{f/+}$; *Math1-Cre*; N=5, *SmoM2*; *Yap* $^{f/f}$; *Taz* $^{f/f}$; *Math1-Cre*). (**E, E'**) Hypertrophic cerebellum driven by SmoM2; *hGFAP-Cre* is not reduced by Yap/Taz loss, even though (**F**, **F'**) efficient *Cre*-mediated deletion is evident at early stages (P1) (N=3, *SmoM2*; *hGFAP-Cre*; N=2, *SmoM2*; *Yap*$^{f/f}$; *hGFAP-Cre*).

*Scale bars: **A, B**: 1mm; **C-F'**: 200μm.

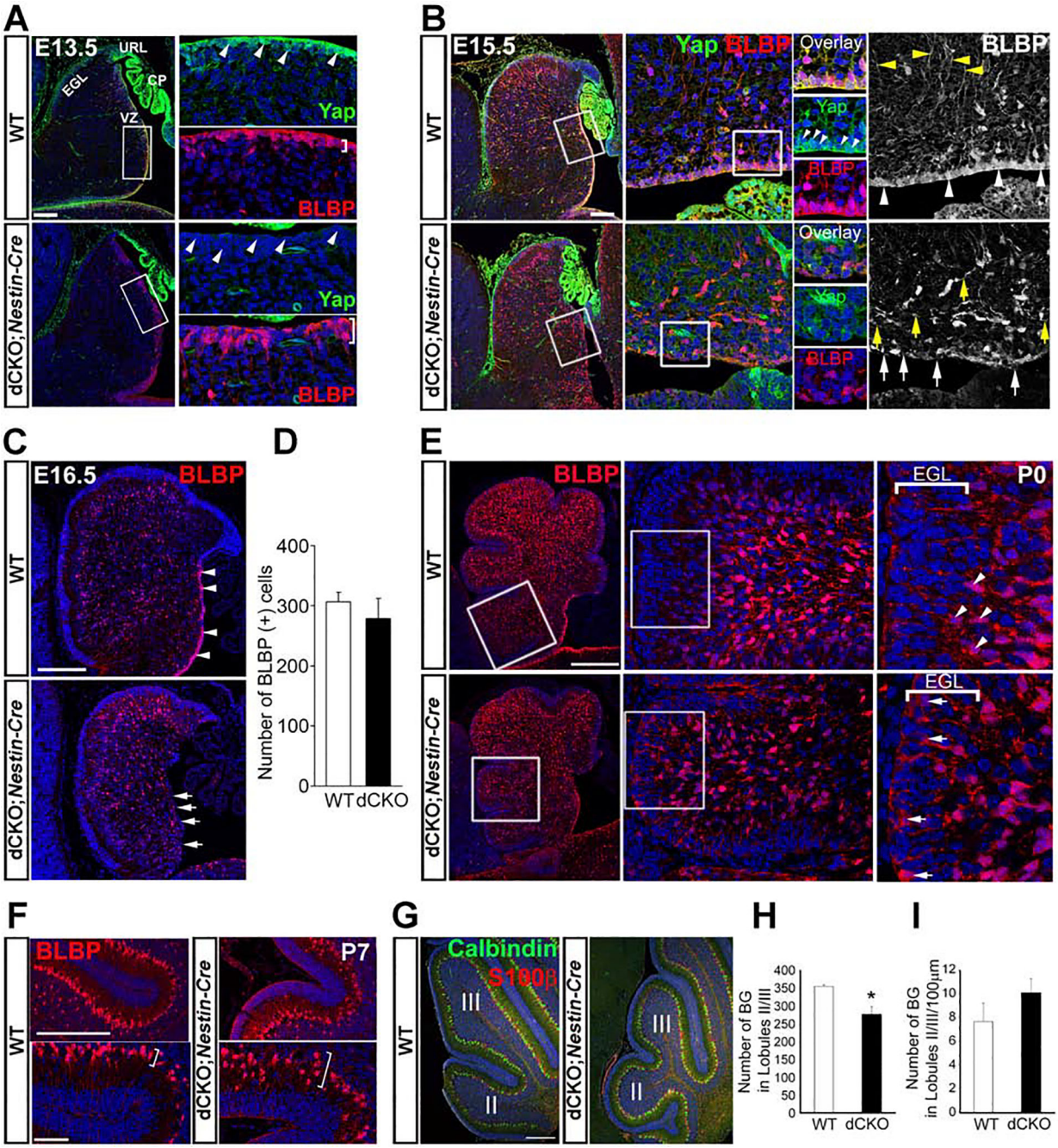

Figure 7. Yap/Taz is necessary for normal shape of radial glia progenitors and BG distribution.

(A) At E13.5, Yap expression is found in the VZ RGPs in the WT but absent in the dCKO; *Nestin-Cre* (arrowheads) and some of the BLBP$^+$ RGPs are less tightly arranged as compared to WT (brackets). **(B)** At E15.5, BLBP$^+$ apical lining RGPs are reduced (arrowheads and arrows) and radial glia processes are randomly distributed in the dCKO compared to dorsally directed processes in the WT (yellow arrowheads and arrows, respectively). **(C)** At E16.5, BLBP$^+$ cells are no longer found in the VZ of dCKO, unlike WT (arrowheads and arrows, respectively). **(D)** Graph comparing the number of BLBP$^+$ cells in the midsagittal section of cerebellum shows that the number of BLBP$^+$ cells does not

differ between WT and dCKO at E16.5 (N=3, p=0.2626). **(E)** At P0, in the anterobasal lobe, $BLBP^+$ cells are more randomly distributed and extend to the EGL in the dCKO (arrows) unlike WT, where most of $BLBP^+$ cells are located in the emerging PCL (arrowheads). **(F)** At P7, around the precentral fissure, $BLBP^+$ cells are more dispersed in the dCKOs compared to WT (brackets). (**G**) At P10, dCKO;*Nestin-Cre* shows smaller lobules I/II and III than WT. **(H)** significantly fewer BG labeled by S100β in lobules II and III compared to WT (p=0.02). (**I**) BG density normalized by the length of PCL does not differ between WT and dCKO (N=3, p=0.11).

*Scale bars: **A, B**: 50 μm, **C:** 100 μm**, E, F, G**: 200 μm, Significance level: $p < 0.05$.

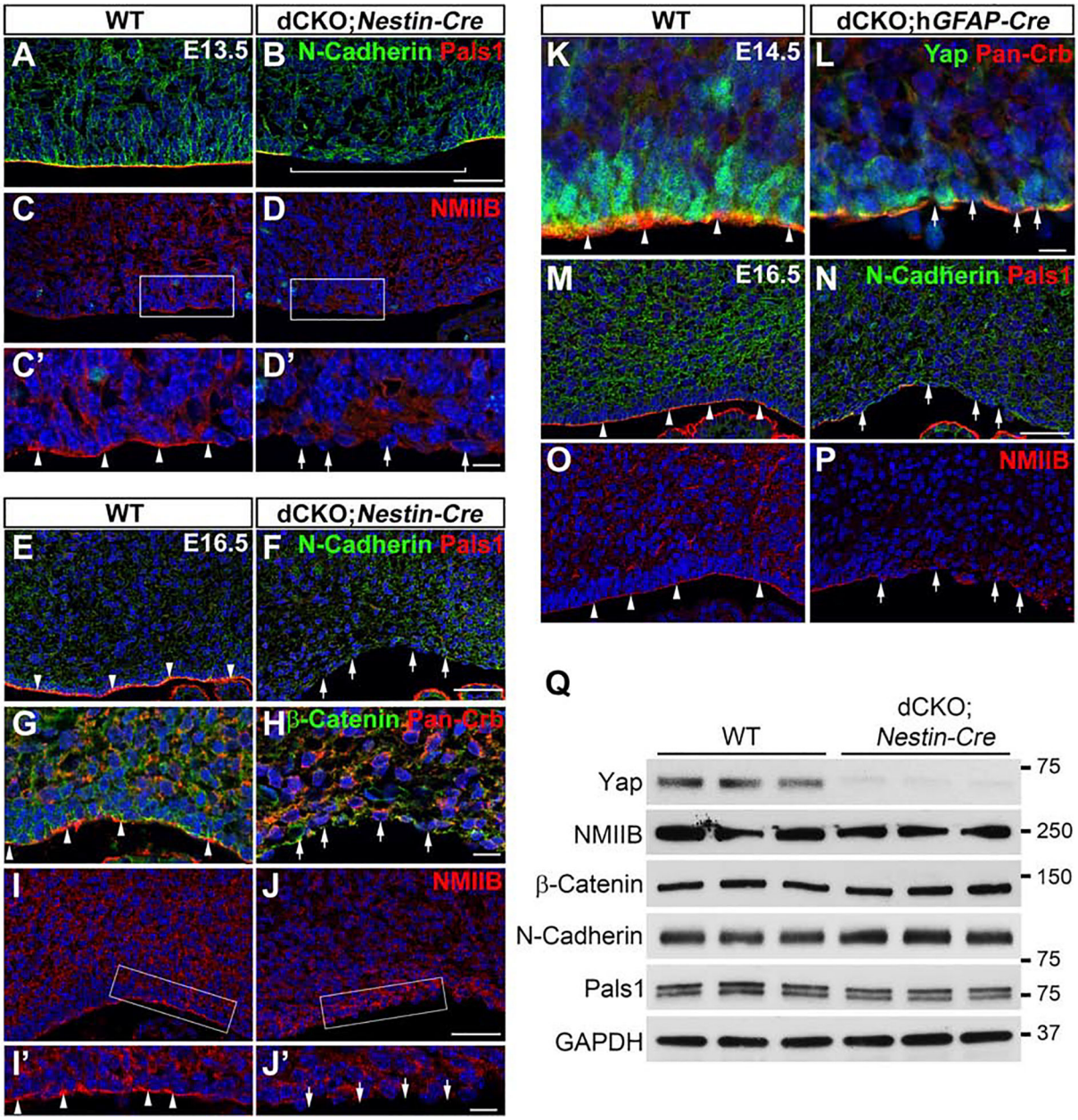

Figure 8. Yap/Taz function is required for the localization of apical junctional components

(A, B) At E13.5, partial loss of AJC complex at the ventricular lining is seen in the dCKO;Nestin-Cre (bracket, **B**) while WT shows the continuous AJC complex (Pals1: apical polarity complex, N-Cadherin: adherens junction) **(A)**. **(C-D')** Similarly, actomyosin component, NMIIB, localization at the apical junction is absent in the dCKO **(C,** arrowheads in **C')** but is well maintained in the WT **(D,** arrows in **D'). (E-H**) At E16.5, polarity complex proteins (Pals1 and Crbs) and N-Cadherin and β-Catenin are no longer localized to the ventricular surface, in contrast to the WT where concentrated distribution is evident (arrowheads and arrows, respectively). **(I-J')** NMIIB localization at the ventricular surface is not found in the dCKO but is intact in the WT. **(K, L)** At E14.5, the dCKO;*hGFAP-Cre* shows the partial reduction of Yap compared to WT, and the loss of apical localization of

Crbs correlates with the Yap-reduced area (arrowheads and arrows, respectively). **(M, N)** At E16.5, the dCKO;*hGFAP-Cre* shows wide areas with loss of Pals1 and N-Cadherin compared to WT (arrows and arrowheads, respectively). **(O, P)** NMIIB localization is also disrupted in wide areas at E16.5 in the dCKO;*hGFAP-Cre* unlike in WT, where continuous apical localization is detected (arrows and arrowheads, respectively). **(Q)** Western blot analyses of whole cerebellum lysates at E15.5 show that substantial reduction of Yap is detected in the dCKO;*Nestin-Cre* but the protein level of AJC components (Pals1, N-Cadherin, β-Catenin, NMIIB) is not obviously different from WT (N=3).
*Scale bars: **A-D, E, F, I, J, M-P**: 50μm; **C', D', I', J', G, H, K, L**: 10μm